α/β-Hydrolase domain-containing 6 (ABHD6) accelerates the desensitization and deactivation of TARP γ-2-containing AMPA receptors

Rixu Cong[1, #], Huiran Li[1, #], Hong Yang[1, #], Jing Gu[1, #], Shanshan Wang[2, #], Xiangyu Guan[1], Tangyunfei Su[1], Yunlin Zheng[3], Dianchun Wang[1], Xinran Chen[1], Lei Yang[1], Yun Stone Shi[7*], Mengping Wei[1*], Chen Zhang[3,4,5,6 *],

[1]School of Basic Medical Sciences, Beijing Key Laboratory of Neural Regeneration and Repair, Advanced Innovation Center for Human Brain Protection, Capital Medical University, Beijing 100069, China.

[2]Peking-Tsinghua Center for Life Sciences, Academy for Advanced Interdisciplinary Studies, Peking University, Beijing 100871, China

[3]School of Basic Medical Sciences, Wenzhou Medical University, Wenzhou, 325035, China.

[4]School of Basic Medical Sciences, Beijing Key Laboratory of Neural Regeneration and Repair, Advanced Innovation Center for Human Brain Protection, Capital Medical University, Beijing 100069, China.

[5]Chinese Institute for Brain Research, Beijing 102206, China.

[6]State Key Laboratory of Translational Medicine and Innovative Drug Development, Jiangsu Simcere Pharmaceutical Co. Ltd, Nanjing 210000, Jiangsu, China.

[7]Ministry of Education Key Laboratory of Model Animal for Disease Study, Model Animal Research Center, Department of Neurology, Nanjing Drum Tower Hospital, Medical School, Nanjing University, Nanjing 210032, China.

[#] Rixu Cong, Huiran Li, Hong Yang, Jing Gu and Shanshan Wang contribute equally to this work.

Running title: ABHD6 accelerates kinetics of the AMPAR-TARP γ-2 complexes

Corresponding author email address

Yun Stone Shi (yunshi@nju.edu.cn), Mengping Wei (weimengping@ccmu.edu.cn), Chen Zhang (czhang@188.con).

ABSTRACT

AMPA receptors (AMPARs) mediate most of the fast excitatory synaptic transmission in mammalian brain. Their efficacy in responding to presynaptic glutamate release depends on their kinetics, which are determined by AMPARs and their auxiliary subunit composition. α/β-Hydrolase domain-containing 6 (ABHD6) is an AMPAR auxiliary subunit that has been shown to negatively regulate the surface delivery of AMPARs and AMPAR-mediated currents. Overexpression of ABHD6 decreased the rising slope and increased the decay τ of mEPSCs. However, whether ABHD6 is involved in regulating AMPAR kinetics remains unclear. Here, we found that ABHD6 per se had no effects on the gating kinetics of GluA1 and GluA2(Q) containing homomeric receptors. However, in the presence of the auxiliary subunit TARP γ-2, ABHD6 accelerated the deactivation and desensitization of either GluA1 and GluA2(Q) containing homomeric receptors independent of their splicing isoforms (flip and flop) and the editing isoforms of GluA2 (R or G at position 764), except the deactivation of GluA2(Q)i-G isoform. Besides, the recovery from desensitization of GluA1 with flip splicing isoform was slowed by the co-expression of ABHD6 in the presence of TARP γ-2. Furthermore, the ABHD6 accelerated the deactivation and desensitization of GluA1i/GluA2(R)i-G heteromeric receptors in the presence of TARP γ-2. Therefore, these results demonstrate that ABHD6 regulates AMPAR gating kinetics in a TARP γ-2-dependent manner.

SIGNIFICANCE STATEMENT

The efficacy of AMPARs in responding to presynaptic glutamate release depends on their kinetics, including deactivation, desensitization, and recovery from desensitization, which are determined by AMPARs and their auxiliary subunit composition. Using ultra-fast application of glutamate and outside-out patch recordings, we found that, in the presence of the auxiliary subunit TARP γ-2, ABHD6 accelerated the deactivation and desensitization of GluA1i/GluA2(R)i-G heteromeric receptors and GluA1 and GluA2(Q) containing homomeric receptors independent of their splicing isoforms (flip and flop) and the editing isoforms of GluA2 (R or G at position 764), except the deactivation of GluA2(Q)i-G isoform. These results demonstrate that ABHD6 regulates AMPAR gating kinetics in a TARP γ-2-dependent manner.

INTRODUCTION

The α-amino-3-hydroxy-5-methyl-4-isoxazolepropionic acid receptors (AMPARs), tetramers consisting of GluA1-4 subunits, are glutamate-gated ion channels that mediate fast excitatory synaptic transmission in the central nervous system (Bredt and Nicoll, 2003; Diering and Huganir, 2018). The transmission strength depends on the number and kinetic characteristics of AMPARs at the postsynaptic membrane (Huganir and Nicoll, 2013). AMPARs exhibit fast kinetics, with activation, deactivation, and desensitization in milliseconds, which enable the rapid depolarization of the postsynaptic membrane, ensuring a high speed and fidelity of signaling in the nervous system to accommodate the speed of information processing in the brain (Erreger et al., 2004; Mayer, 2005; Luscher and Malenka, 2012; Greger et al., 2017). AMPAR kinetics not only affects synaptic transmission and plasticity, but also neurotoxicity through Ca^{2+} permeability (Huganir and Nicoll, 2013; Diering and Huganir, 2018; Yang et al., 2021). Abnormalities in AMPAR kinetics disrupt synaptic signaling and neuronal homeostasis, which are associated with a range of neurological disorders, such as Alzheimer's disease, epilepsy, amyotrophic lateral sclerosis, and

stroke (Qneibi et al., 2019; Yang et al., 2021).

In the brain, auxiliary subunits are found to assemble with AMPARs with different stoichiometries, and modulate AMPAR kinetics (Kato et al., 2008; Brockie and Maricq, 2010; Cheng et al., 2012; Schwenk et al., 2012; Shanks NF, 2012; Yang et al., 2014; Matt et al., 2018). TARP γ-2 was the first auxiliary subunit to be discovered. This subunit positively regulates AMPAR functions, such as promoting affinity, increasing surface expression, slowing deactivation and desensitization, and accelerating recovery from desensitization (Gill et al., 2011; Chen et al., 2017). Besides, other auxiliary proteins have also been reported to modulate AMPAR kinetics. CNIH-2 slows the deactivation and desensitization of GluA1i/A2(R) in *Xenopus* oocytes but has no effect on its recovery from desensitization, while it slows the deactivation and desensitization of GluA1i and accelerates its recovery from desensitization in HEK 293T cells. GSG1L slows AMPAR deactivation, desensitization, and recovery from desensitization in *Xenopus* oocytes and HEK cells (Kato et al., 2010; Khodosevich et al., 2014; Jacobi and von Engelhardt, 2017). This diversity results from coassembly of the known AMPAR subunits, pore-forming GluA and three types of auxiliary proteins, with 21 additional constituents, mostly secreted proteins or transmembrane proteins of different classes. Their integration at distinct abundance and stability establishes the heteromultimeric architecture of native AMPAR complexes: a defined core with a variable periphery resulting in an apparent molecular mass between 0.6 and 1 MDa (Schwenk et al., 2012; Khodosevich et al., 2014). Studies have found that TARP γ-8 and CNIH2 could bound to the same AMPARs complex, and compared to existence of TARP γ-8 alone with GluA1, the time course of AMPAR deactivation and decreased desensitization decreased with CNIH-2 affiliated. And the binding sites for these two families (TARPs and CNIHs) of transmembrane proteins are distinct (Shi et al., 2010). Besides, using cryo-electron microscopy (cryo-EM), studies showed that TARP γ-8 and CNIH2 can assemble in the same AMPAR complex (Yu et al., 2021).

ABHD6 is a member of the α/β-hydrolase family. It was previously reported to be a

serine hydrolase that could control 2-arachidonoylglycerol (2-AG) levels at cannabinoid receptors, plays a critical role in 2-AG signaling in endocannabinoid signaling system (Chevaleyre et al., 2006; Marrs et al., 2010). High-resolution proteomic analysis has shown that ABHD6 is associated with the natural AMPAR core subunit (Schwenk et al., 2012). Functional studies revealed that overexpression of ABHD6 drastically reduced AMPAR-mediated currents by selectively inhibits the surface expression levels of AMPARs without altering total expression levels of AMPARs. The effects of ABHD6 on AMPARs was observed in both neurons and heterologous cells (Wei et al., 2016; Wei et al., 2017). Wei et al. also tested whether the observed effects was due to ABHD6's hydrolase activity. Using the specific inhibitor of ABHD6 lipase activity, WWL70, or the lipase activity deficit mutation (S148A) of ABHD6, they found that the effects was independent of ABHD6's hydrolase activity. Using two-dimensional gel separation of the ER and membrane fractions, Schwenk and colleagues demonstrated the assembly of AMPARs in ER and their delivery to plasma membrane (Schwenk et al., 2019). They showed ABHD6 trapped GluAs in the monomeric GluA-ABHD6 complex, and thus eliminated tetramer formation and surface delivery of AMPARs. In addition to this, overexpression of ABHD6 significantly increased the decay τ of mEPSCs in cultured hippocampal neurons, which indicated that ABHD6 may affect the kinetics of AMPARs (Wei et al., 2016; Wei et al., 2017). However, whether and how ABHD6 regulates AMPAR kinetics remain unknown. In this study, we investigated whether ABHD6 plays a regulatory role in the kinetic properties of functional AMPARs and whether this role is subject to AMPAR RNA editing and splice variants differences. Following previous studies (Priel et al., 2005; Milstein et al., 2007; Kato et al., 2008; Gill et al., 2011; Khodosevich et al., 2014), we transfected different GluAs, GluAs + ABHD6, GluAs + TARP γ-2, GluAs + TARP γ-2 + ABHD6 in HEK 293T cells, and systematically studied their channel properties. Our data showed that ABHD6 did not affect the kinetic properties of AMPARs. However, in the presence of TARP γ-2, ABHD6 accelerated the deactivation and desensitization of TARP γ-2 containing GluA1 and GluA2(Q) homomeric receptors independent of their splicing isoforms

142 and editing isoforms, except the deactivation of GluA2(Q)i-G isoform, and the
143 deactivation and desensitization of GluA1i/GluA2(R)i-G heteromeric receptors. Our
144 findings revealed a new function of ABHD6 in regulating the channel properties
145 TARP γ-2-containing AMPA receptors.

RESULTS

ABHD6 reduced the glutamate-induced currents mediated by AMPARs in the presence and absence of TARP γ-2

Previous studies have shown that ABHD6 can significantly decrease currents in HEK 293T cells transfected with GluA1i, GluA2(R)i, GluA3i, GluA1i+GluA2(R)i, GluA2(R)i+GluA3i, or GluA2(R)i+GluA3i in the presence or absence of TARP γ-2 (Wei et al., 2016; Wei et al., 2017; Schwenk et al., 2019). However, whether ABHD6 inhibits other RNA editing and splice variants of AMPARs remains unclear. To answer this question, we constructed a total of 14 isoforms of GluA1, GluA2, and GluA3, specifically GluA1i, GluA1o, GluA2(Q)i-R, GluA2(Q)o-R, GluA2(Q)i-G, GluA2(Q)o-G, GluA2(R)i-R, GluA2(R)o-R, GluA2(R)i-G, GluA2(R)o-G, GluA3i-R, GluA3o-R, GluA3i-G, and GluA3o-G (illustrated in Fig. 1 A and Fig. EV1). We recorded glutamate-induced currents in HEK 293T cells transfected with these variants together with ABHD6 or control plasmid. Our results showed that ABHD6 overexpression decreased the peak amplitudes of the currents mediated by GluA1i to ~34%, GluA1o to ~48%, GluA2(Q)i-R to ~31%, GluA2(Q)o-R to ~32%, GluA2(Q)i-G to ~45%, and GluA2(Q)o-G to ~21% (Fig. 1 B-C, Table. EV1.1, EV1.2). We also recorded the currents of these variants in the presence of TARP γ-2. TARP γ-2 increased GluA1- and GluA2-induced currents, but its effect on the increase in GluA3-induced currents was not significant, which is generally consistent with previous studies reporting a small effect of TARP γ-2 on GluA3 currents (Pei et al., 2007; Coleman et al., 2016). Moreover, ABHD6 overexpression decreased the peak amplitudes of currents mediated by GluA1i to ~14%, GluA1o to ~37%, GluA2(Q)i-R to ~9%, GluA2(Q)o-R to ~11%, GluA2(Q)i-G to ~6%, GluA2(Q)o-G to ~7%, GluA2(R)i-R to ~10%, GluA2(R)o-R to ~44%, GluA2(R)i-G to ~11%, GluA2(R)o-G to ~21%, GluA3i-R to ~5%, GluA3o-R to ~38%, GluA3i-G to ~21%, and GluA3o-G to ~24%, in the presense of TARP γ-2 (Fig. 1 B-D, Table. EV1.1, EV1.2). Taken together, these results showed that ABHD6 significantly reduced the glutamate-induced currents mediated by AMPARs in the pre- or ab-sence of TARP γ-2

175 independently of the subunit type, flip/flop splice variants, and Q/R or R/G RNA
176 editing.

177 **ABHD6 accelerated the deactivation of homomeric AMPAR-TARP γ-2**
178 **complexes.**

179 To investigate whether ABHD6 affected AMPAR deactivation in the pre- or ab-sence
180 of TARP γ-2, we transfected HEK 293T cells with GluAs (GluA1i, GluA1o,
181 GluA2(Q)i-R, GluA2(Q)o-R, GluA2(Q)i-G, GluA2(Q)o-G, GluA1i/GluA2(R)i),
182 GluAs + ABHD6, GluAs + TARP γ-2, and GluAs + ABHD6 + TARP γ-2. 1-ms
183 application of 10 mM glutamate could induce the receptor deactivation, a rapidly
184 activated inward current followed by rapid decay to baseline levels, under outside-out
185 patch recordings (-60 mV). Concerning about impact of GluA expression levels on the
186 membrane on the current kinetics, we conducted Pearson correlation analyses between
187 the amplitude and kinetics of the currents from various glutamate receptor assemblies
188 we measured, results showed that there is no correlation between peak amplitude and
189 kinetics of AMPARs (Fig. EV6). Consistent with previous observations, our data
190 showed that TARP γ-2 slowed AMPAR deactivation without selective differences in
191 subunits, splice variants, or RNA editing (Fig. 2). Moreover, ABHD6 overexpression
192 had a negligible effect on the deactivation of AMPARs, including GluA1i, GluA1o,
193 GluA2(Q)i-R, GluA2(Q)o-R, GluA2(Q)i-G, and GluA2(Q)o-G (Fig. 2 A-F, Fig. EV2
194 A-F, Table. EV2.1, EV2.2). However, ABHD6 overexpression reduced the
195 deactivation time constant ($\tau_{w,\ deac}$) of AMPAR in the presence of TARP γ-2, except
196 for GluA2(Q)i-G (Fig. 2 A-F, Fig. EV2 A-F, Table. EV2.1, EV2.2). Specifically,
197 ABHD6 significantly decreased the $\tau_{w,\ deact}$ of GluA1i to ~48%, of GluA1o to ~65%,
198 of GluA2(Q)i-R to ~48%, of GluA2(Q)o-R to ~60%, and of GluA2(Q)o-G to ~60% in
199 the presence of TARP γ-2 (Fig. 2 A-F, Fig. EV2 A-F, Table. EV2.1, EV2.2).
200 Next, we wonder whether the observed phenotype was due to the effects of ABHD6
201 on TARPed AMPARs, or due to the changes of the ratio of TARPed and unTARPed
202 receptors under our experimental condition. First of all, to avoid that the observed
203 phenotype was due to the changes of the ratio of TARPed to unTARPed AMPARs

following ABHD6 overexpression, we constructed chimera plasmids that fused GluA2(Q)i-R or GluAi and TARP γ-2 together. We recorded the deactivation using outside-out patch recordings (- 60 mV), and examined whether ABHD6 could affect its kinetics. We found that overexpression of ABHD6 decreased the peak amplitudes of the currents of GluA2(Q)i-R-TARP γ-2 to ~23%, and GluA1i-TARP γ-2 to ~25%, and accelerated $\tau_{w,\ deact}$ mediated by GluA2(Q)i-R-TARP γ-2 to ~65% or GluA1i-TARP γ-2 to ~55% (Fig. 2G, 2I, Fig. EV2G, 2I, Table. EV2.1, EV2.2). These results are consistent with our previous findings using two plasmids to express AMPARs and TARP γ-2. Secondly, we isolated TARP γ-2-containing AMPA receptors using the method of Carbone et al., Nature Communications, 2016, in which they added 50 μM spermine to the internal solution and recorded at + 50 mV. We transfected chimera plasmids GluA2(Q)i-R-TARP γ-2 or GluA1i-TARP γ-2 together with ABHD6 or control plasmid, and recorded the deactivation of AMPA receptors at + 50 mV in the presence of 50 μM spermine. Our results showed that ABHD6 could still decreased the peak amplitudes of currents and accelerated the $\tau_{w,\ deact}$ mediated by GluA2(Q)i-R-TARP γ-2 or GluA1i-TARP γ-2 (Fig. 2H, 2J, Fig. EV2H, 2J, Table. EV2.1, EV2.2). Taken together, our results clearly show that ABHD6 could affect the gating kinetics of TARPed AMPARs.

Collectively, these results showed that ABHD6 accelerated the deactivation of TARP γ-2-containing AMPARs, except for the GluA2(Q)i-G variants.

ABHD6 accelerated the desensitization of homomeric AMPAR-TARP γ-2 complexes

To investigate whether ABHD6 affected AMPAR desensitization, we recorded the desensitization induced by a 100-ms application of 10 mM glutamate using outside-out patch recordings (-60 mV). The desensitization curve showed a slow decay pattern than deactivation due to the long-term action of glutamate. ABHD6 overexpression had an insignificant effect on the desensitization of AMPARs, including GluA1i, GluA1o, GluA2(Q)i-R, GluA2(Q)o-R, GluA2(Q)i-G, and GluA2(Q)o-G (Fig. 3 A-F, Fig. EV3 A-F, Table. EV3.1, EV3.2). We also studied the effects of ABHD6 on the

desensitization in the presence of TARP γ-2. Consistent with previous observations, our data showed that TARP γ-2 slowed AMPAR desensitization without selective differences in subunits, splice variants, or RNA editing (Priel et al., 2005; Coombs et al., 2012; Devi et al., 2020). ABHD6 overexpression reduced the desensitization time constant ($\tau_{w, des}$) of AMPARs in the presence of TARP γ-2. Specifically, it significantly decreased the $\tau_{w, des}$ of GluA1i to ~62%, of GluA1o to ~63%, of GluA2(Q)i-R to ~59%, of GluA2(Q)o-R to ~65%, of GluA2(Q)i-G to ~60%, and of GluA2(Q)o-G to ~71% (Fig. 3 A-F, Fig. EV3 A-F, Table. EV3.1, EV3.2) in the presence of TARP γ-2.

To further confirm that the observed phenotype of ABHD6 on AMPAR desensitization was due to the effect of ABHD6 on TARPed AMPARs, we also tried the chimera plasmids that fused GluA2(Q)i-R or GluAi and TARP γ-2 together as we did in deactivation studies. We found that overexpression of ABHD6 accelerated $\tau_{w, des}$ mediated by GluA2(Q)i-R-TARP γ-2 or GluA1i-TARP γ-2 (Figure 3G, 3I, Figure EV3G, 3I, Table. EV3.1, EV3.2). Besides, we added 50 μM spermine to the internal solution and recorded at +50 mV to isolated TARPed receptors, and found that ABHD6 could still accelerated the $\tau_{w, des}$ mediated by GluA2(Q)i-R-TARP γ-2 or GluA1i-TARP γ-2 (Figure 3H, 3J, Figure EV3H, 3J, Table. EV3.1, EV3.2).

Collectively, these results showed that ABHD6 accelerated the desensitization of TARP γ-2-containing AMPARs and that the effect did not depend on differences in GluA1/2(Q) subunits, flip/flop splice variants, or R/G editing.

ABHD6 slowed the recovery of homomeric GluA1i-TARP γ-2 complexes from desensitization

Recovery from desensitization is another important parameter of AMPAR channel kinetics. To investigate whether ABHD6 affected AMPAR recovery from desensitization, we recorded the recovery curve in the presence or absence of TARP γ-2. Using outside-out patch recordings (-60 mV), we performed 100-ms paired-pulse stimulation at different intervals (stimulation was performed at intervals of 1-601 ms) to plot the recovery ratio curve. Consistent with previous studies, our data showed that TARP γ-2 accelerated GluA1 recovery from desensitization (Fig. 4 A-B, Fig. EV4 A-

262 B, Table. EV4.1, EV4.2). Moreover, it accelerated GluA2(Q)i but not GluA2(Q)o
263 recovery (Fig. 4 C-F, Fig. EV4 C-F, Table. EV4.1, EV4.2). We also found that
264 ABHD6 overexpression had little effect on the recovery of AMPARs in the presence
265 or absence of TARP γ-2, except for GluA1i-TARP γ-2, whose recovery from
266 desensitization time constant (τ_{rec}) increased to ~157% (Fig. 4 A, Fig. EV4 A, Table.
267 EV4.1, EV4.2). We confirmed this results using chimera GluA2(Q)i-R-TARP γ-2 and
268 GluA1i-TARP γ-2 plasmid, and found that ABHD6 overexpression increased the τ_{rec}
269 of GluA1i-TARP γ-2 to ~135%, without changing the τ_{rec} of GluA2(Q)i-R-TARP γ-2
270 (Fig. 4 G-H, Fig. EV4 G-H, Table. EV4.1, EV4.2). These results showed that the
271 GluA1i-TARP γ-2 complex played a specific role in the regulation of AMPAR
272 recovery from desensitization by ABHD6. The recovery of flip splice variants was
273 more susceptible to regulation by other auxiliary subunits.

274 **ABHD6 negatively regulates the kinetics of heteromeric GluA1i/GluA2(R)i-G-**
275 **TARP γ-2 complexes**

276 To investigate whether affected kinetic properties of native receptor subtypes in near-
277 physiological states, we performed additional experiments using heteromeric
278 receptors. Previous studies have shown that diheteromeric GluA1/GluA2 and
279 GluA2/GluA3 receptors are the most common sets in the mammalian brain, especially
280 in the mouse hippocampus where the diheteromeric GluA1/GluA2 occupies more
281 than 50% of the calcium-impermeable AMPA receptor complexes (Wenthold et al.,
282 1996; Lu et al., 2009; Zhao et al., 2019; Yu et al., 2021). Following previous studies
283 (Cho et al., 2007; Schwenk et al., 2009; Schwenk et al., 2012; Herring et al., 2013;
284 Klaassen et al., 2016), We co-transfected GluA1i/GluA2(R)i-G, GluA1i/GluA2(R)i-
285 G+ABHD6, GluA1i/GluA2(R)i-G+ TARP γ-2, GluA1i/GluA2(R)i-G+ TARP γ-
286 2+ABHD6 in HEK 293T cells (GluA1i: GluA2(R)i-G: TARP γ-2 : ABHD6=0.4 μg :
287 0.4 μg : 1.2 μg : 30 ng). And we recorded the deactivation and desensitization and
288 recovery as previously described using outside-out patch recordings (-60 mV).
289 Consistent with previous studies (Schwenk et al., 2009; Coombs et al., 2012), our data
290 showed that TARP γ-2 increased the peak amplitude of currents mediated by

GluA1i/GluA2(R)i-G receptors, slowed the deactivation and desensitization of GluA1i/GluA2(R)i-G receptors and accelerated its recovery (Fig. 5, Fig. EV5, Table. EV5.1, EV5.2). Our results showed that ABHD6 only accelerated the deactivation and desensitization of TARP γ-2-containing GluA1i/GluA2(R)i-G receptors, $\tau_{w,\ deact}$ and $\tau_{w,\ des}$ of GluA1i/GluA2(R)i-G–TARP γ-2 to ~62% and ~55% respectively (Fig. 5A, 5B, Table. EV5.1, EV5.2). However, ABHD6 overexpression decreased the currents and slowed its recovery in the presence and absence of TARP γ-2. Specifically, ABHD6 significantly decreased the peak amplitudes of currents mediated by GluA1i/GluA2(R)i-G receptor to ~62%, of GluA1i/GluA2(R)i-G-TARP γ-2 to ~17%. ABHD6 increased the τ_{rec} of GluA1i/GluA2(R)i-G and GluA1i/GluA2(R)i-G–TARP γ-2 to ~203% and ~198% (Fig. 5C, Fig. EV5, Table. EV5.1, EV5.2).

DISCUSSION

In this study, we systematically studied the effects of ABHD6 on the amplitudes and kinetics of AMPARs with different subunit types, GluA1(flip/flop), GluA2(Q) (flip/flop, R/G) and diheteromeric GluA1i/GluA2(R)i-G receptors, in the presence or absence of TARP γ-2 in HEK 293T cells. Our results showed that ABHD6 inhibited glutamate-induced currents in all different AMPARs. ABHD6 regulated the gating kinetics of AMPARs in the presence of TARP γ-2.

Previous studies have reported that ABHD6 can reduce glutamate-induced currents and the surface expression of GluAs independently of the subunit composition (Wei et al., 2016; Wei et al., 2017). They found that ABHD6 overexpression can reduce AMPAR-currents and surface expression levels of AMPARs in HEK 293T cells transfected with GluA1i, GluA2(R)i, GluA3i, GluA1i+GluA2(R)i, GluA2(R)i+GluA3i, or GluA2(R)i+GluA3i in the presence or absence of TARP γ-2. In addition to flip splice of AMPAR subunits, mammalian brains also have the flop splicing isoform. The flop splice variants are expressed in a pattern that differs from but partially overlaps with flip splice variants. The CA1 and CA3 regions of the hippocampus predominantly express flip splice variants, whereas DG highly

expresses flop splice variants (Sommer et al., 1990). Flip splice variants remain unchanged in the developing brain since birth, whereas flop splice variants are expressed at low levels in the first eight days of life and reach adult levels by day 14, suggesting that flop splice variants may be involved in the formation of mature receptors (Monyer et al., 1991). Q/R editing enables the conversion of neutral to positively charged residues in the ion-selective filter of the channel, causing impermeability to divalent cations (mainly Ca^{2+}), which not only affects the current and conductance of the channel but also plays an important role in neuronal functional impairment and excitotoxicity (Kawahara et al., 2004; Kwak and Kawahara, 2004). Our results showed that ABHD6 also inhibited currents in HEK 293T cells transfected with flop splice variants and R/G editing. Thus, this study provided further evidence that ABHD6 inhibited AMPARs on the amplitude of glutamate-induced currents. The reason for the decreased AMPAR-mediated currents might be due to the negative effects of ABHD6 on the tetramer formation of AMPARs reported by Schwenk J and colleagues (Schwenk et al., 2019).

AMPARs bind to multiple auxiliary subunits simultaneously, and the interactions between subunits directly influence the kinetic characteristics of AMPARs. TARP γ-2, TARP γ-3, TARP γ-4, and TARP γ-8 slow the deactivation and desensitization of GluA1i-containing AMPARs in HEK 293T cells (Cho et al., 2007; Milstein et al., 2007). TARP γ-5 accelerates not only AMPAR deactivation and desensitization in HEK 293T cells but also desensitization after transfection into neurons (Kato et al., 2008). Studies have shown that in *Xenopus* oocytes and HEK cells, GSG1L slows GluA1i/2i and GluA2(Q)i deactivation, desensitization, and recovery from desensitization and blocks the slowing effect of CNIH-2 on deactivation and desensitization (Schwenk et al., 2012; Shanks NF, 2012; Kamalova et al., 2020). GSG1L slows the kinetics of recombinant AMPARs in heterologous cells but accelerates those of natural AMPARs in CA1 pyramidal neurons when overexpressed in cultured organotypic hippocampal slices. Moreover, it slows the kinetics of CA1 pyramidal neurons in acute slices from knockout rats, which may be influenced by

349 AMPAR subunit composition/chemometrics, posttranslational modifications, and
350 auxiliary subunits in neurons superimposed on the co-expression of subunits (Gu et
351 al., 2016; Mao et al., 2017). CNIH-2 and CNIH-3 slow GluA1i/ A2(R)i-G and
352 GluA2(R)o-G/A4o-R deactivation and desensitization in *Xenopus* oocytes (Schwenk
353 et al., 2009; Schwenk et al., 2012), as well as GluA1i, GluA2(Q)i, and GluA1i/A2(R)i
354 deactivation and GluA1i desensitization in tsA201 and HEK 293T cells (Kato et al.,
355 2010; Gill et al., 2011; Coombs et al., 2012). CNIH-3 overexpression slows AMPAR
356 desensitization in cultured rat optic nerve oligodendrocyte precursor cells (Coombs et
357 al., 2012), but CNIH-2 overexpression does not affect AMPAR kinetics in
358 hippocampal pyramidal neurons and cerebellar granule neurons (Shi et al., 2010).
359 Furthermore, CNIHs interact with TARPs. TARP γ-8 blocks the slowing effect of
360 CNIH-2 on GluA2 but not GluA1 deactivation in HEK 293T cells (Herring et al.,
361 2013). SynDIG4 can also slow GluA1i/GluA2(R)i deactivation and synergize with
362 TARP γ-8, but does not affect GluA1/GluA2 heterodimer desensitization (Matt et al.,
363 2018). CKAMP44 overexpression slows deactivation, accelerates desensitization, and
364 slows recovery from desensitization, while CKAMP44 knockout has no effect on
365 either deactivation or desensitization (Khodosevich et al., 2014; von Engelhardt,
366 2019). In this study, we systematically studies how ABHD6 affected the kinetic
367 characteristics of AMPARs. In CA1 pyramidal neurons' synapses, the major form of
368 AMPAR's are heteromeric receptors that consisted of GluA2 with the other subunits
369 (Malinow and Malenka, 2002; Bredt and Nicoll, 2003; Shepherd and Huganir, 2007).
370 However, previous studies also found poorly expressed but significant population of
371 GluA1 homomeric receptors in the hippocampus (Wenthold et al., 1996; Sans and
372 C.Y., 2003). In addition, Zhao et al. studied the molecular structures of native
373 AMPARs by cyro-EM, and elucidated the structure of 10 forms of native AMPARs
374 which includes A2A2A2A2 homomeric form (Zhao et al., 2016). Thus, we studied the
375 effect of ABHD6 on the kinetic characteristics of either homomeric AMPARs or
376 heteromeric AMPARs. Our results clearly demonstrated that, unlike previously
377 identified auxiliary subunits, ABHD6 accelerates GluA1 and GluA2(Q) deactivation

and desensitization in the presence but not in the absence of TARP γ-2，which are also consistent with the previous publication that overexpression of ABHD6 accelerates AMPARs mediated deactivation in neurons (Wei et al., 2017). The results may suggest a novel mechanism by which auxiliary subunits regulate the kinetics of AMPARs and their ability not to regulate the kinetics of GluAs but to alter the kinetics of native AMPARs by altering the stoichiometry of TARPs in the AMPARs complex. Moreover, its effects do not depend on the flip/flop isoform or R/G editing of AMPARs. We did not investigate the effects of ABHD6 on the kinetics of GluA2 Q607R–edited and GluA3-related AMPARs because their glutamate-induced currents are not detectable.

There are still questions that need to be answered. Whether ABHD6 also affects AMPAR kinetics in endogenously knocked out or overexpressed neurons? And what are the molecular mechanisms behind the role of ABHD6 in regulating AMPAR kinetics in a TARP γ-2-dependent manner? The structure of the AMPARs-TARP γ-2 complex has revealed that the TMD of TARP γ-2 is arranged around the TMD of AMPARs and serves to support the ion channel pore of the receptor (Chen et al., 2017; Zhao et al., 2019). When AMPARs are activated, the differentially charged extracellular region of TARP γ-2 binds to the LBD of AMPARs, stabilizes the intra- and inter-dimeric interfaces of AMPARs, regulates the activation, deactivation and desensitization of AMPARs (Tomita et al., 2005; Zhao et al., 2016). Previous studies have shown the binding of ABHD6 to the CTD of AMPARs through pull down experiments (Wei et al., 2017). However, the CTD structure of TARP γ-2 and AMPARs has not been reported. Further structure-based studies may provide more information about the channel gating properties of AMPARs.

403 **MATERIALS AND METHODS**

404 **Construction of expression vectors**

405 Cloning of mouse ABHD6-2A-GFP containing pFUGW was performed as previously
406 described. GluA1-3 cDNA (rat) applied to plasmid construction as previously
407 described(Wei et al., 2017; Jiang et al., 2021). The flip and flop isoforms were cloned
408 into an IRES-GFP expression vector using polymerase chain reaction (PCR). Q/R and
409 R/G editing variants were generated using PCR. Seventeen plasmids of GluA were
410 constructed: GluA1i, GluA1o, GluA2(Q)i-R, GluA2(Q)o-R, GluA2(Q)i-G,
411 GluA2(Q)o-G, GluA2(R)i-R, GluA2(R)o-R, GluA2(R)i-G, GluA2(R)o-G, GluA3i-R,
412 GluA3o-R, GluA3i-G, GluA3o-G, GluA1i-γ-2, GluA2(Q)i-R-γ-2 and
413 GluA1i/GluA2(R)i-G.

414 **HEK 293T cell culture and transfection**

415 HEK 293T cells were cultured in Dulbecco's Modified Eagle Medium (Gibco)
416 containing 10% fetal bovine serum (ExCell Bio) and 1% penicillin–streptomycin
417 (Gibco) in an incubator with 5% CO^2 at 37 ℃. The transfection reagent used was
418 polyethylenimine (Polysciences)(Chai et al., 2017; Wang et al., 2023; Wei et al.,
419 2024). The weight ratio of the GluA, TARP γ-2, and ABHD6 plasmids was 2:3:0.3125
420 (the GluA plasmid was 0.8 μg/well). Transfection was terminated 3 h after initiation.
421 HEK 293T cells were dissociated with 0.05% trypsin and then placed on poly-D-
422 lysine-coated coverslips. To prevent cell toxicity due to AMPARs transfection, 200
423 μM NBQX (Abcam) was added to the culture medium after transfection. The
424 transfected cells were grown for > 18 h before electrophysiology recording.

425 **Outside-out patch recording**

426 Recordings were obtained using an EPC 10 patch clamp (HEKA). The data were
427 digitized at 10 kHz. Unless otherwise stated, the holding potential was −60 mV, and
428 series resistance compensation was set to 60–80%, and recordings with series
429 resistances >20 MΩ or the Ileak > -200 pA were rejected. The cells were continuously

perfused with an external solution containing 150 mM NaCl, 4 mM KCl, 2 mM $CaCl_2$, 1 mM $MgCl_2$, 10 mM HEPES, and 10 mM glucose at pH 7.4 and Osm 315. Electrodes with a resistance of 4–6 MΩ were pulled from borosilicate glass capillaries (WPI). The internal solution contained 125 mM KF, 33 mM KOH, 2 mM $MgCl_2$, 1 mM $CaCl_2$, 11 mM EGTA, and 10 mM HEPES at pH 7.4 and Osm 310, and 50 μM spermine was added when indicated. Solutions containing L-glutamate (Sigma-Aldrich) were applied by patch membrane perfusion with θ tubes driven by a piezo manipulator (HVA). Glutamate (10 mM) pulses of 1 or 100 ms were applied every 5 s. To calculate the weighted time constant, time constant of deactivation ($\tau_{w,\ deact}$) and time constant of desensitization ($\tau_{w,\ des}$) were fitted according to a double exponential function. For AMPAR recovery from desensitization, two-pulse (10 mM glutamate; 100 ms) stimulation was performed at intervals of 1–601 ms. To allow full recovery from desensitization, the sweeps were separated by 5 s. The current evoked by the preceding stimulus was defined as 1, while the other was defined as 2. The recovery ratio was calculated as follows:

$$Recovery\ ratio\ (\%) = \left(I_{Peak} - I_{steady-state}\right)_2 / \left(I_{Peak} - I_{steady-state}\right)_1$$

The time constant of recovery from desensitization (τ_{rec}) was calculated using nonlinear one-phase exponential decay fitting.

Statistical analysis

The data were analyzed using Clampfit 9.02 (Molecular Devices), Igor Pro 6.0 (WaveMetrics), and Prism 8 (GraphPad Software). Data normality was assessed using the D'Agostino–Pearson omnibus normality test. Statistical differences were examined using one-way ANOVA for normally distributed data or a nonparametric test otherwise. Correlation was examined using Pearson correlation analysis. Values of $P < 0.05$ were considered statistically significant.

Acknowledgments: This work was supported by grants from National Key R&D Program of China [2017YFA0105201]; the National Science Foundation of China

[81925011, 92149304, 32170954, 32100763, and 31900698]; Key-Area Research and Development Program of Guangdong Province [2019B030335001]; The Youth Beijing Scholars Program [015], Support Project of High-level Teachers in Beijing Municipal Universities [CIT&TCD20190334]; Beijing Advanced Innovation Center for Big Data-based Precision Medicine, Capital Medical University, Beijing, China [PXM2021_014226_000026].

Author contributions: R.C., H.L., H.Y., J.G., L.Y., M.W., and C.Z. designed the research; R.C., H.L., H.Y., J.G., S.W. and M.W. conducted the research and analyzed the data; X.G., T.S., Y.Z., D.W. and X.C. analyzed the data; M.W. and C.Z. wrote the paper.

Competing interests: The authors declare that they have no conflicts of interest.

References

Bredt DS, Nicoll RA (2003) AMPA Receptor Trafficking at Excitatory Synapses. Neuron 40:361-379.

Brockie PJ, Maricq AV (2010) In a Pickle: Is Cornichon Just Relish or Part of the Main Dish? Neuron 68:1017-1019.

Chai Z, Wang C, Huang R, Wang Y, Zhang X, Wu Q, Wang Y, Wu X, Zheng L, Zhang C, Guo W, Xiong W, Ding J, Zhu F, Zhou Z (2017) CaV2.2 Gates Calcium-Independent but Voltage-Dependent Secretion in Mammalian Sensory Neurons. Neuron 96:1317-1326.e1314.

Chen S, Zhao Y, Wang Y, Shekhar M, Tajkhorshid E, Gouaux E (2017) Activation and Desensitization Mechanism of AMPA Receptor-TARP Complex by Cryo-EM. Cell 170:1234-1246.e1214.

Cheng J, Dong J, Cui Y, Wang L, Wu B, Zhang C (2012) Interacting Partners of AMPA-Type Glutamate Receptors. Journal of Molecular Neuroscience 48:441-447.

Chevaleyre V, Takahashi KA, Castillo PE (2006) Endocannabinoid-Mediated Synaptic Plasticity in the Cns. Annual Review of Neuroscience 29:37-76.

Cho C-H, St-Gelais F, Zhang W, Tomita S, Howe JR (2007) Two Families of TARP Isoforms that Have Distinct Effects on the Kinetic Properties of AMPA Receptors and Synaptic Currents. Neuron 55:890-904.

Coleman SK, Hou Y, Willibald M, Semenov A, Möykkynen T, Keinänen K (2016) Aggregation Limits Surface Expression of Homomeric GluA3 Receptors. Journal of Biological Chemistry 291:8784-8794.

Coombs ID, Soto D, Zonouzi M, Renzi M, Shelley C, Farrant M, Cull-Candy SG (2012) Cornichons Modify Channel Properties of Recombinant and Glial AMPA Receptors. Journal of Neuroscience 32:9796-9804.

Devi SPS, Cheng Y, Tomita S, Howe JR, Zhang W (2020) TARPs Modulate Receptor-Mediated Paired-Pulse Depression and Recovery from Desensitization. The Journal of Neuroscience 40:8233-8247.

Diering GH, Huganir RL (2018) The AMPA Receptor Code of Synaptic Plasticity. Neuron 100:314-329.

Erreger K, Chen PE, Wyllie DJA, Traynelis PSF (2004) Glutamate Receptor Gating. Critical Reviews in Neurobiology 16:187-224.

Gill MB, Kato AS, Wang H, Bredt DS (2011) AMPA receptor modulation by cornichon‐2 dictated by transmembrane AMPA receptor regulatory protein isoform. European Journal of Neuroscience 35:182-194.

Greger IH, Watson JF, Cull-Candy SG (2017) Structural and Functional Architecture of AMPA-Type Glutamate Receptors and Their Auxiliary Proteins. Neuron 94:713-730.

Gu X, Mao X, Lussier MP, Hutchison MA, Zhou L, Hamra FK, Roche KW, Lu W (2016) GSG1L suppresses AMPA receptor-mediated synaptic transmission and uniquely modulates AMPA receptor kinetics in hippocampal neurons. Nature Communications 7.

Herring Bruce E, Shi Y, Suh Young H, Zheng C-Y, Blankenship Sabine M, Roche Katherine W, Nicoll Roger A (2013) Cornichon Proteins Determine the Subunit Composition of Synaptic AMPA Receptors. Neuron 77:1083-1096.

Huganir Richard L, Nicoll Roger A (2013) AMPARs and Synaptic Plasticity: The Last 25 Years. Neuron 80:704-717.

Jacobi E, von Engelhardt J (2017) Diversity in AMPA receptor complexes in the brain. Current Opinion in Neurobiology 45:32-38.

515 Jiang C-H, Wei M, Zhang C, Shi YS (2021) The amino-terminal domain of GluA1 mediates LTP
516 maintenance via interaction with neuroplastin-65. Proceedings of the National Academy of
517 Sciences 118.
518 Kamalova A, Futai K, Delpire E, Nakagawa T (2020) AMPA Receptor Auxiliary Subunit GSG1L
519 Suppresses Short-Term Facilitation in Corticothalamic Synapses and Determines Seizure
520 Susceptibility. Cell Reports 32.
521 Kato AS, Siuda ER, Nisenbaum ES, Bredt DS (2008) AMPA Receptor Subunit-Specific Regulation by
522 a Distinct Family of Type II TARPs. Neuron 59:986-996.
523 Kato AS, Gill MB, Ho MT, Yu H, Tu Y, Siuda ER, Wang H, Qian Y-W, Nisenbaum ES, Tomita S, Bredt
524 DS (2010) Hippocampal AMPA Receptor Gating Controlled by Both TARP and Cornichon
525 Proteins. Neuron 68:1082-1096.
526 Kawahara Y, Ito K, Sun H, Aizawa H, Kanazawa I, Kwak S (2004) Glutamate receptors RNA editing
527 and death of motor neurons. Nature 427:801-801.
528 Khodosevich K, Jacobi E, Farrow P, Schulmann A, Rusu A, Zhang L, Sprengel R, Monyer H,
529 von Engelhardt J (2014) Coexpressed Auxiliary Subunits Exhibit Distinct Modulatory Profiles
530 on AMPA Receptor Function. Neuron 83:601-615.
531 Klaassen RV, Stroeder J, Coussen F, Hafner A-S, Petersen JD, Renancio C, Schmitz LJM, Normand E,
532 Lodder JC, Rotaru DC, Rao-Ruiz P, Spijker S, Mansvelder HD, Choquet D, Smit AB (2016)
533 Shisa6 traps AMPA receptors at postsynaptic sites and prevents their desensitization during
534 synaptic activity. Nature Communications 7.
535 Kwak S, Kawahara Y (2004) Deficient RNA editing of GluR2 and neuronal death in amyotropic lateral
536 sclerosis. Journal of Molecular Medicine 83:110-120.
537 Lu W, Shi Y, Jackson AC, Bjorgan K, During MJ, Sprengel R, Seeburg PH, Nicoll RA (2009) Subunit
538 Composition of Synaptic AMPA Receptors Revealed by a Single-Cell Genetic Approach.
539 Neuron 62:254-268.
540 Luscher C, Malenka RC (2012) NMDA Receptor-Dependent Long-Term Potentiation and Long-Term
541 Depression (LTP/LTD). Cold Spring Harbor Perspectives in Biology 4:a005710-a005710.
542 Malinow R, Malenka RC (2002) AMPA Receptor Trafficking and Synaptic Plasticity. Annual Review
543 of Neuroscience 25:103-126.
544 Mao X, Gu X, Lu W (2017) GSG1L regulates the strength of AMPA receptor-mediated synaptic
545 transmission but not AMPA receptor kinetics in hippocampal dentate granule neurons. Journal
546 of Neurophysiology 117:28-35.
547 Marrs WR et al. (2010) The serine hydrolase ABHD6 controls the accumulation and efficacy of 2-AG
548 at cannabinoid receptors. Nature Neuroscience 13:951-957.
549 Matt L, Kirk LM, Chenaux G, Speca DJ, Puhger KR, Pride MC, Qneibi M, Haham T, Plambeck KE,
550 Stern-Bach Y, Silverman JL, Crawley JN, Hell JW, Díaz E (2018) SynDIG4/Prrt1 Is Required
551 for Excitatory Synapse Development and Plasticity Underlying Cognitive Function. Cell
552 Reports 22:2246-2253.
553 Mayer ML (2005) Glutamate receptor ion channels. Current Opinion in Neurobiology 15:282-288.
554 Milstein AD, Zhou W, Karimzadegan S, Bredt DS, Nicoll RA (2007) TARP Subtypes Differentially and
555 Dose-Dependently Control Synaptic AMPA Receptor Gating. Neuron 55:905-918.
556 Monyer H, Seeburg PH, Wisden W (1991) Glutamate-operated channels: Developmentally early and
557 mature forms arise by alternative splicing. Neuron 6:799-810.
558 Pei W, Huang Z, Niu L (2007) GluR3 Flip and Flop: Differences in Channel Opening Kinetics.

Biochemistry 46:2027-2036.
Priel A, Kolleker A, Ayalon G, Gillor M, Osten P, Stern-Bach Y (2005) Stargazin Reduces Desensitization and Slows Deactivation of the AMPA-Type Glutamate Receptors. The Journal of Neuroscience 25:2682-2686.
Qneibi M, Hamed O, Fares O, Jaradat N, Natsheh A-R, AbuHasan Q, Emwas N, Al-Kerm R, Al-Kerm R (2019) The inhibitory role of curcumin derivatives on AMPA receptor subunits and their effect on the gating biophysical properties. European Journal of Pharmaceutical Sciences 136.
Sans N, Vissel, B., Petralia, R.S., Wang, Y.X., Chang, K., Royle, G.A., Wang,, C.Y. OG, S., Heinemann, S.F., and Wenthold, R.J (2003) Aberrant formation of glutamate receptor complexes in hippocampal neurons of mice lacking the GluR2 AMPA recept. J Neurosci 23: 9367–9373.
Schwenk J, Harmel N, Zolles G, Bildl W, Kulik A, Heimrich B, Chisaka O, Jonas P, Schulte U, Fakler B, Klöcker N (2009) Functional Proteomics Identify Cornichon Proteins as Auxiliary Subunits of AMPA Receptors. Science 323:1313-1319.
Schwenk J, Harmel N, Brechet A, Zolles G, Berkefeld H, Müller Catrin S, Bildl W, Baehrens D, Hüber B, Kulik A, Klöcker N, Schulte U, Fakler B (2012) High-Resolution Proteomics Unravel Architecture and Molecular Diversity of Native AMPA Receptor Complexes. Neuron 74:621-633.
Schwenk J, Boudkkazi S, Kocylowski MK, Brechet A, Zolles G, Bus T, Costa K, Kollewe A, Jordan J, Bank J, Bildl W, Sprengel R, Kulik A, Roeper J, Schulte U, Fakler B (2019) An ER Assembly Line of AMPA-Receptors Controls Excitatory Neurotransmission and Its Plasticity. Neuron 104:680-692.e689.
Shanks NF SJ, Maruo T, Cais O, Hirao A, Oe S, Ghosh A, Noda Y, Greger IH, Yates JR, 3rd, Nakagawa T (2012) Differences of AMPA and kainate receptor interactomes identify a novel AMPA receptor auxiliary subunit, GSG1L. Cell reports 1:590-598.
Shepherd JD, Huganir RL (2007) The Cell Biology of Synaptic Plasticity: AMPA Receptor Trafficking. Annual Review of Cell and Developmental Biology 23:613-643.
Shi Y, Suh YH, Milstein AD, Isozaki K, Schmid SM, Roche KW, Nicoll RA (2010) Functional comparison of the effects of TARPs and cornichons on AMPA receptor trafficking and gating. Proceedings of the National Academy of Sciences 107:16315-16319.
Sommer B, Keinänen K, Verdoorn TA, Wisden W, Burnashev N, Herb A, Kohler M, Takagi T, Sakmann B, Seeburg PH (1990) Flip and Flop: A Cell-Specific Functional Switch in Glutamate-Operated Channels of the CNS. Science 249:1580-1585.
Tomita S, Adesnik H, Sekiguchi M, Zhang W, Wada K, Howe JR, Nicoll RA, Bredt DS (2005) Stargazin modulates AMPA receptor gating and trafficking by distinct domains. Nature 435:1052-1058.
von Engelhardt J (2019) AMPA Receptor Auxiliary Proteins of the CKAMP Family. International Journal of Molecular Sciences 20.
Wang X, Zheng W, Zhu Z, Xing B, Yan W, Zhu K, Xiao L, Yang C, Wei M, Yang L, Jin Z-B, Bi X, Zhang C (2023) Timp1 Deletion Induces Anxiety-like Behavior in Mice. Neuroscience Bulletin.
Wei M, Jia M, Zhang J, Yu L, Zhao Y, Chen Y, Ma Y, Zhang W, Shi YS, Zhang C (2017) The Inhibitory Effect of α/β-Hydrolase Domain-Containing 6 (ABHD6) on the Surface Targeting of GluA2- and GluA3-Containing AMPA Receptors. Frontiers in Molecular Neuroscience 10.

Wei M, Yang L, Su F, Liu Y, Zhao X, Luo L, Sun X, Liu S, Dong Z, Zhang Y, Shi YS, Liang J, Zhang C (2024) ABHD6 drives endocytosis of AMPA receptors to regulate synaptic plasticity and learning flexibility. Progress in Neurobiology 233.

Wei M, Zhang J, Jia M, Yang C, Pan Y, Li S, Luo Y, Zheng J, Ji J, Chen J, Hu X, Xiong J, Shi Y, Zhang C (2016) α/β-Hydrolase domain-containing 6 (ABHD6) negatively regulates the surface delivery and synaptic function of AMPA receptors. Proceedings of the National Academy of Sciences 113.

Wenthold RJ, Petralia RS, Blahos J, II, Niedzielski AS (1996) Evidence for multiple AMPA receptor complexes in hippocampal CA1/CA2 neurons. The Journal of Neuroscience 16:1982-1989.

Yang X, Hou D, Jiang W, Zhang C (2014) Intercellular protein–protein interactions at synapses. Protein & Cell 5:420-444.

Yang Y, Okada S, Sakurai M (2021) Adenosine-to-inosine RNA editing in neurological development and disease. RNA Biology 18:999-1013.

Yu J, Rao P, Clark S, Mitra J, Ha T, Gouaux E (2021) Hippocampal AMPA receptor assemblies and mechanism of allosteric inhibition. Nature 594:448-453.

Zhao Y, Chen S, Yoshioka C, Baconguis I, Gouaux E (2016) Architecture of fully occupied GluA2 AMPA receptor–TARP complex elucidated by cryo-EM. Nature 536:108-111.

Zhao Y, Chen S, Swensen AC, Qian W-J, Gouaux E (2019) Architecture and subunit arrangement of native AMPA receptors elucidated by cryo-EM. Science 364:355-362.

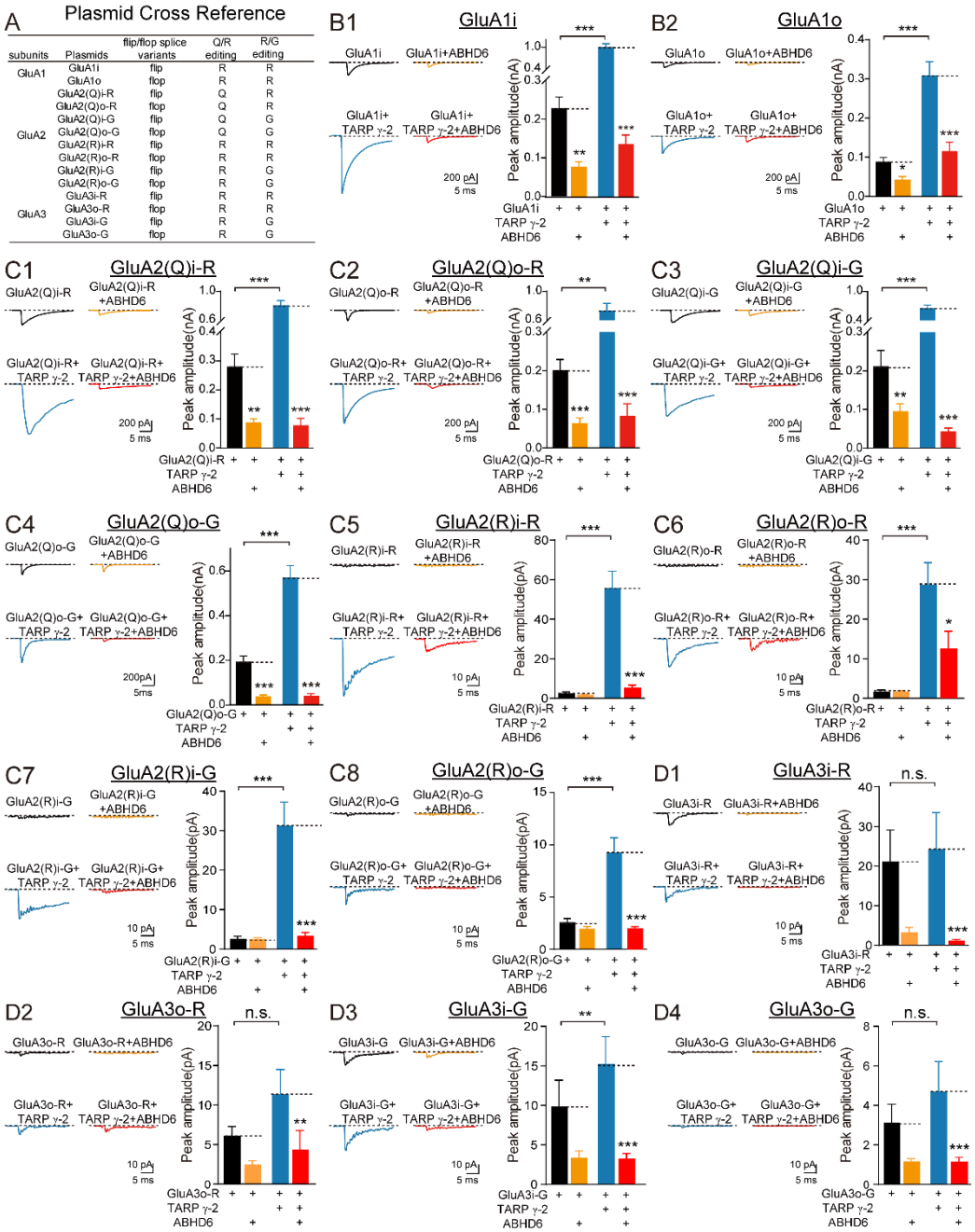

Figure 1. the Effect of overexpression of ABHD6 on the reduction of peak current in AMPARs.

(A) Plasmid abbreviations and variant combinations of AMPAR.

(B-D) Representative traces (left) and summary graphs of the peak amplitudes (right) of 10 mM glutamate-induced currents in HEK 293T cells transfected with GluA1-3 (black), GluA1-3 + ABHD6 (orange), GluA1-3 + TARP γ-2 (blue), GluA1-3 + TARP γ-2 + ABHD6 (red).

The statistical method was one-way ANOVA followed by a two-way comparison (*$P < 0.05$; **$P < 0.01$; ***$P < 0.001$. Table. EV1.2).

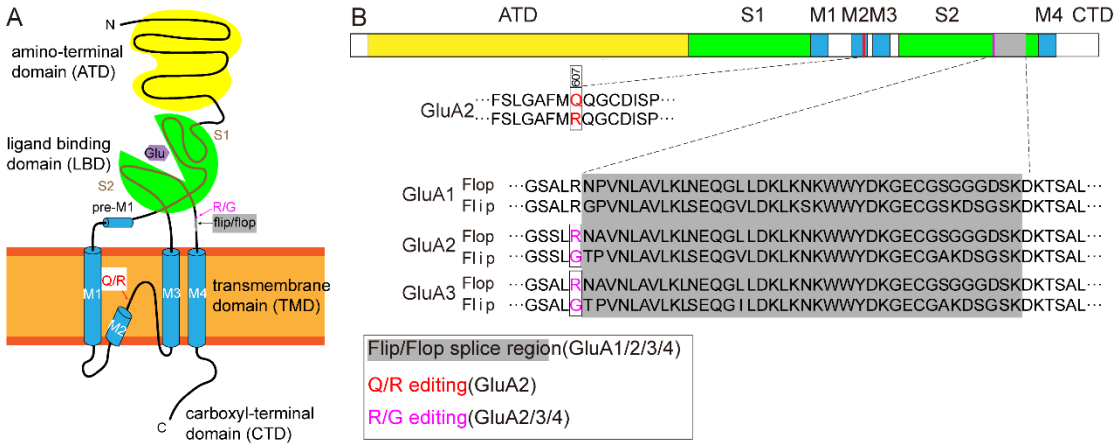

Figure EV1. Schematic illustration of the AMPAR subunit and the Sequence alignment of RNA splice variants and editing of AMPAR.

(A) Topology of a single AMPAR subunit in the plasma membrane. Each subunit consists of an extracellular N-terminal domain (NTD), a ligand-binding domains (LBD), a transmembrane domain (TMD, M1–4) and an intracellular C-terminal domain (CTD), the flip/flop splice variants and the RNA editing sites (Q/R and R/G) are also shown.

(B) Sequence alignment of RNA splice variants and editing. Q/R editing sites (red letters) (GluA2), R/G editing sites (purple letters) (GluA2, A3), flip/flop splice variants (Grey box) (GluA1–A3). Complete sequences can be found in UniProt. Sequences are homologous and conserved in mouse, rat and human.

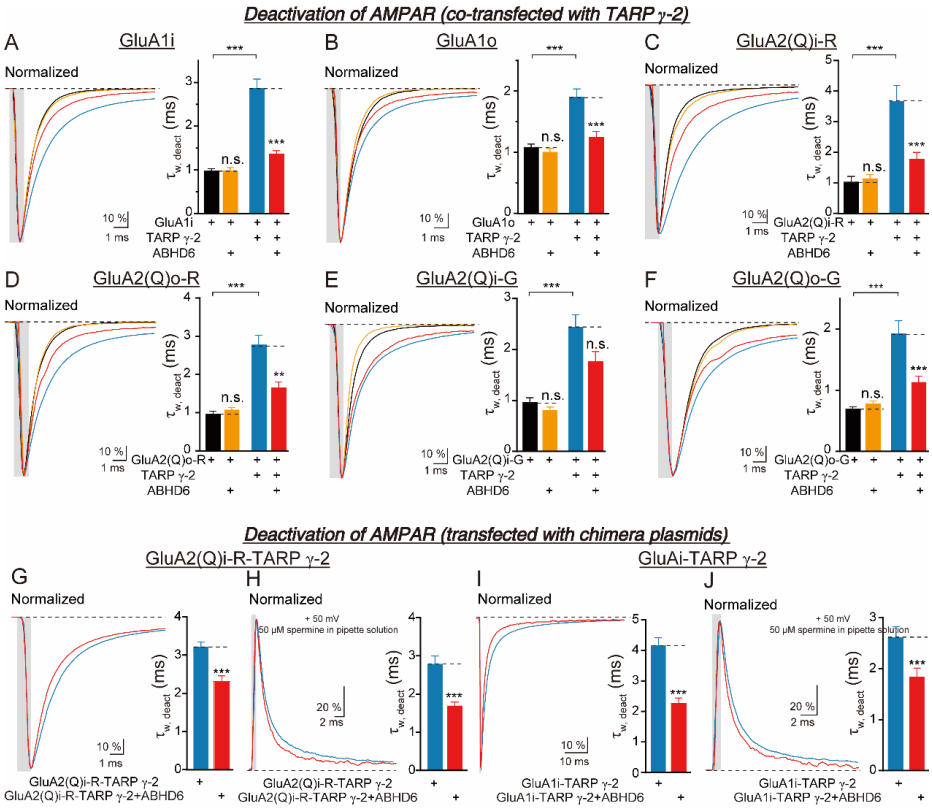

649

650 **Figure 2. Overexpression of ABHD6 accelerated the deactivation of AMPARs-**
651 **TARP γ-2 complexes in HEK 293T cells.**

652 The normalized traces, and the summary bar graphs of the $\tau_{w,\,deact}$ of Glutamate (10
653 mM Glu, 1 ms) induced currents in the outside-out patch from HEK 293T cells
654 transfected with GluA (black), GluA + ABHD6 (orange), GluA + TARP γ-2 (blue),
655 and GluA + TARP γ-2 + ABHD6 (red). (A) GluA1i. (B) GluA1o. (C) GluA2(Q)i-R.
656 (D) GluA2(Q)o-R. (E) GluA2(Q)i-G. (F) GluA2(Q)o-G. (G) GluA2(Q)i-R-TARP γ-2
657 tandem. (I) GluA1i-TARP γ-2 tandem. γ2-containing GluA receptors could be isolated
658 when 50 μM spermine in the internal solution and recorded at +50 mV, the average
659 traces and the normalized traces (right), and the summary bar graphs of the $\tau_{w,\,deact}$ of
660 Glutamate (10 mM Glu, 1 ms) induced currents in the outside-out patch recorded at
661 +50 mV from HEK 293T cells transfected with GluA-TARP γ-2 tandem (blue), GluA-
662 TARP γ-2 tandem + ABHD6 (red). (H) GluA2(Q)i-R-TARP γ-2. (J) GluA1i-TARP γ-
663 2. The statistical method was one-way ANOVA followed by a two-way comparison
664 (*$P < 0.05$; **$P < 0.01$; ***$P < 0.001$. Table. EV2.2).

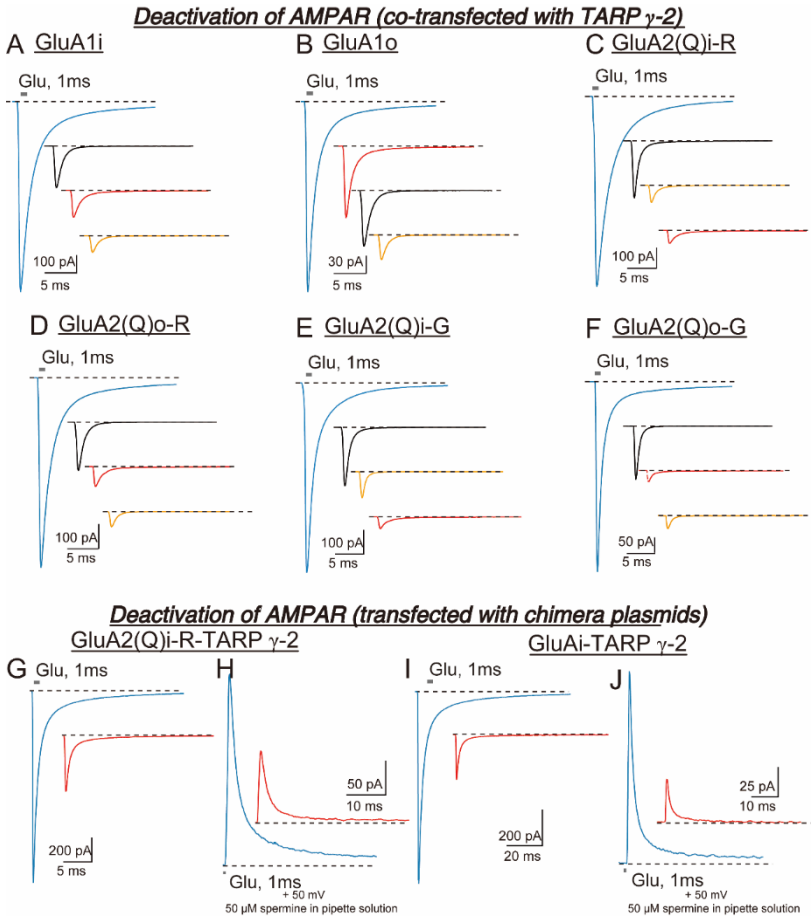

Figure EV2. Average traces of deactivation of AMPAR with overexpression of ABHD6 in HEK 293T cells.

The average traces of Glutamate (10 mM Glu, 1 ms) induced currents in the outside-out patch from HEK 293T cells transfected with GluA (black), GluA + ABHD6 (orange), GluA + TARP γ-2 (blue), and GluA + TARP γ-2 + ABHD6 (red). (A) GluA1i. (B) GluA1o. (C) GluA2(Q)i-R. (D) GluA2(Q)o-R. (E) GluA2(Q)i-G. (F) GluA2(Q)o-G. (G, H) GluA2(Q)i-R-TARP γ-2 tandem. (I, J) GluA1i-TARP γ-2 tandem.

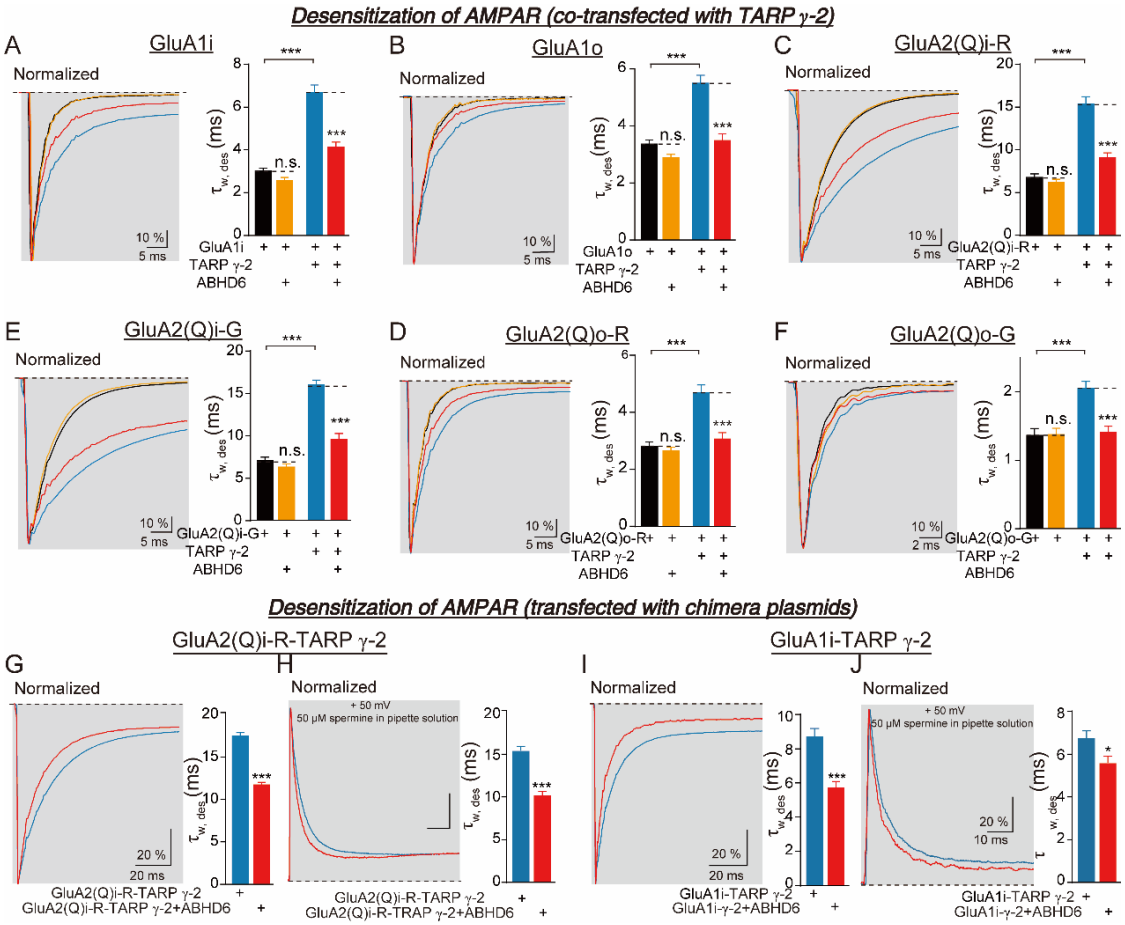

675

676 **Figure 3. Overexpression of ABHD6 accelerated the desensitization of AMPARs-**
677 **TARP γ-2 complexes in HEK 293T cells.**

678 The normalized traces, and the summary bar graphs of the $\tau_{w, des}$ of Glutamate (10
679 mM Glu, 100 ms) induced currents in the outside-out patch from HEK 293T cells
680 transfected with GluA (black), GluA + ABHD6 (orange), GluA + TARP γ-2 (blue),
681 and GluA + TARP γ-2 + ABHD6 (red).(A) GluA1i. (B) GluA1o. (C) GluA2(Q)i-R.
682 (D) GluA2(Q)o-R. (E) GluA2(Q)i-G. (F) GluA2(Q)o-G. (G) GluA2(Q)i-R-TARP γ-2
683 tandem. (I) GluA1i-TARP γ-2 tandem. TARP γ-2-containing GluA receptors could be
684 isolated when 50 μM spermine in the internal solution and recorded at +50 mV, the
685 average traces and the normalized traces (right), and the summary bar graphs of the τ
686 $_{w, des}$ and peak amplitude of Glutamate (10 mM Glu, 100 ms) induced currents in the
687 outside-out patch recorded at +50 mV from HEK 293T cells transfected with GluA-
688 TARP γ-2 tandem (blue), GluA-TARP γ-2 tandem + ABHD6 (red). (H) GluA2(Q)i-R-

TARP γ-2. (J) GluA1i-TARP γ-2. The statistical method was one-way ANOVA followed by a two-way comparison (*$P < 0.05$; **$P < 0.01$; ***$P < 0.001$. Table. EV3.2).

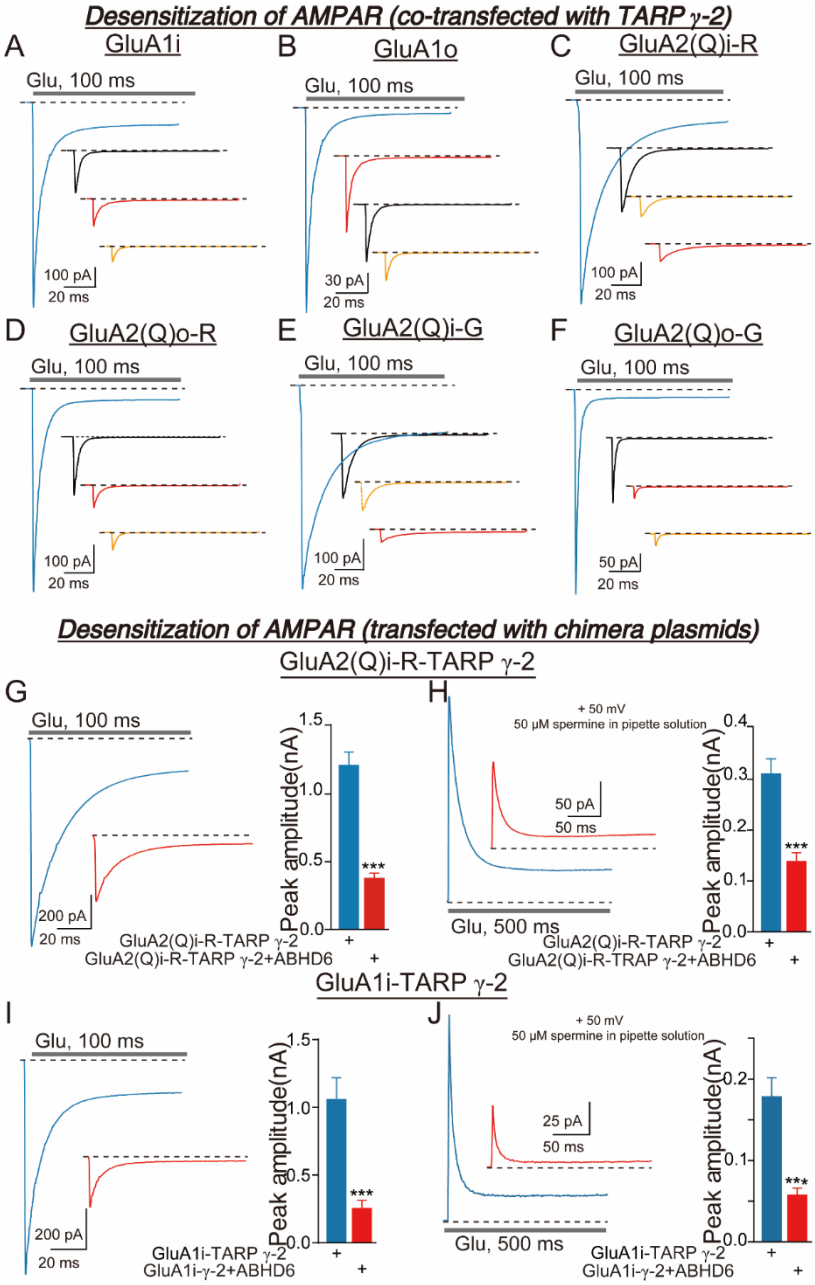

Figure EV3. Average traces of desensitization of AMPAR with overexpression of ABHD6 in HEK 293T cells.

The average traces of Glutamate (10 mM Glu, 500 ms) induced currents in the outside-out patch from HEK 293T cells transfected with GluA (black), GluA + ABHD6 (orange), GluA + TARP γ-2 (blue), and GluA + TARP γ-2 + ABHD6 (red). (A) GluA1i. (B) GluA1o. (C) GluA2(Q)i-R. (D) GluA2(Q)o-R. (E) GluA2(Q)i-G. (F) GluA2(Q)o-G. (G, H) GluA2(Q)i-R-TARP γ-2 tandem. (I, J) GluA1i-TARP γ-2

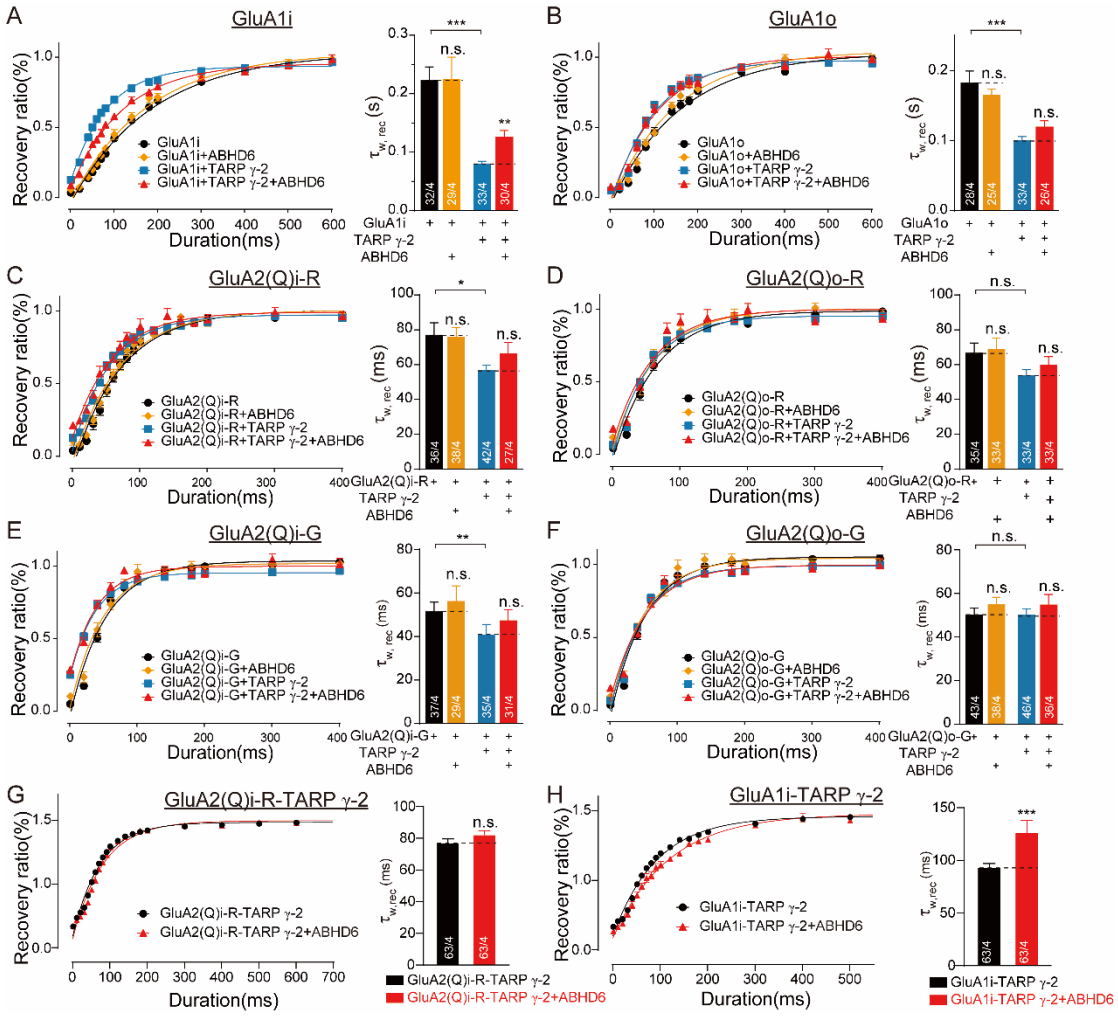

tandem.

Figure 4. Overexpression of ABHD6 slows the recovery from desensitization of GluA1i-TARP γ-2 complexes in HEK 293T cells.

(A-F) Glutamate (Glu, 10 mM) induced currents in an outside-out patch excised from an HEK 293T cell transfected with GluA (black), GluA + ABHD6 (orange), GluA + TARP γ-2 (blue), and GluA+ TARP γ-2 + ABHD6 (red). The recovery ratio curves from desensitization, and the summary bar graphs of the $\tau_{w, rec.}$ (A) GluA1i. (B) GluA1o. (C) GluA2(Q)i-R. (D) GluA2(Q)o-R. (E) GluA2(Q)i-G. (F) GluA2(Q)o-G. (G) GluA2(Q)i-R-TARP γ-2 tandem. (H) GluA1i-TARP γ-2 tandem. The statistical method was one-way ANOVA followed by a two-way comparison (*$P < 0.05$; **$P < 0.01$; ***$P < 0.001$. Table. EV4.2).

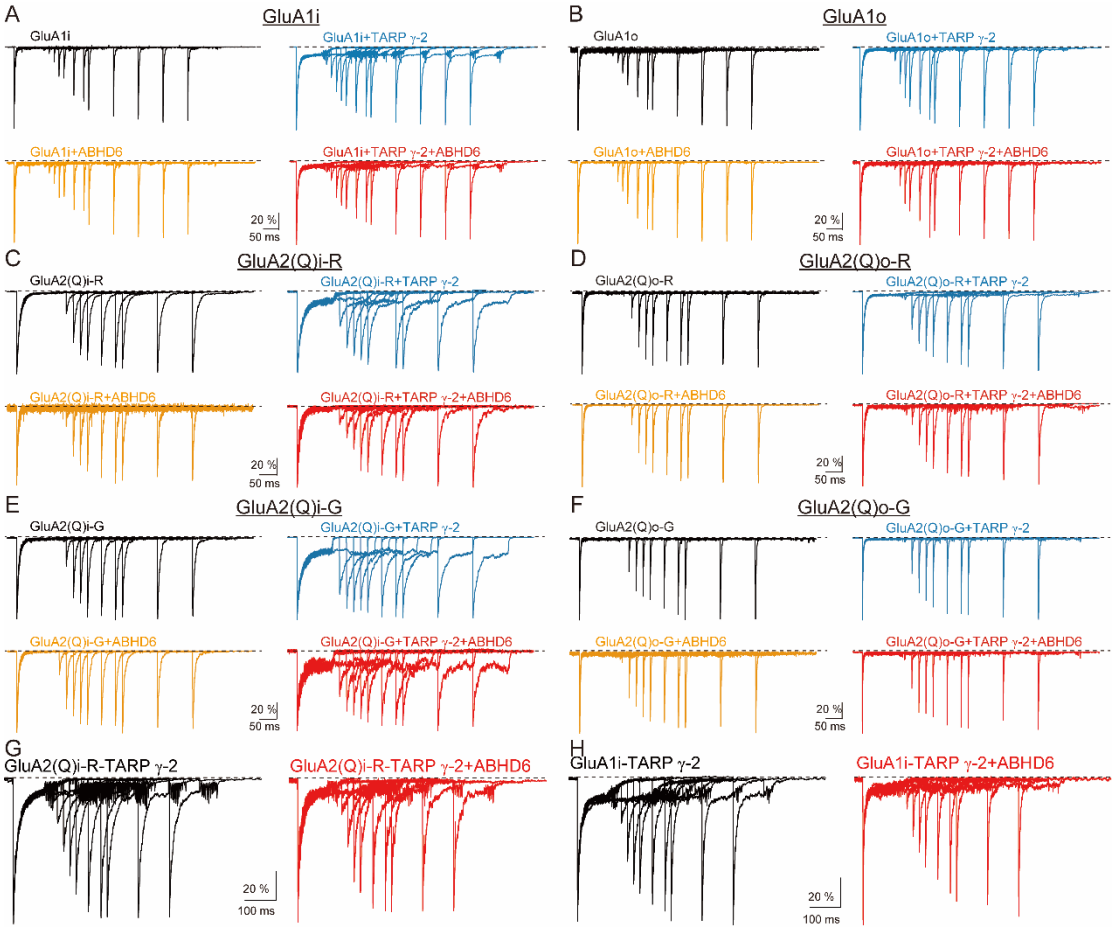

Figure EV4. Typical traces of the recovery from desensitization of AMPAR in HEK 293T cells.

(A-F) Glutamate (Glu, 10 mM) induced currents in an outside-out patch excised from an HEK 293T cell transfected with GluA (black), GluA + ABHD6 (orange), GluA + TARP γ-2 (blue), and GluA+ TARP γ-2 + ABHD6 (red). The first application of 100 ms glutamate was followed by a second glutamate application at increasing pulse intervals at -60 mV. The typical traces from a cell are normalized and aligned to the peak. The typical traces of the recovery from desensitization. (A) GluA1i. (B) GluA1o. (C) GluA2(Q)i-R. (D) GluA2(Q)o-R. (E) GluA2(Q)i-G. (F) GluA2(Q)o-G. (G) GluA2(Q)i-R-TARP γ-2 tandem. (H) GluA1i-TARP γ-2 tandem.

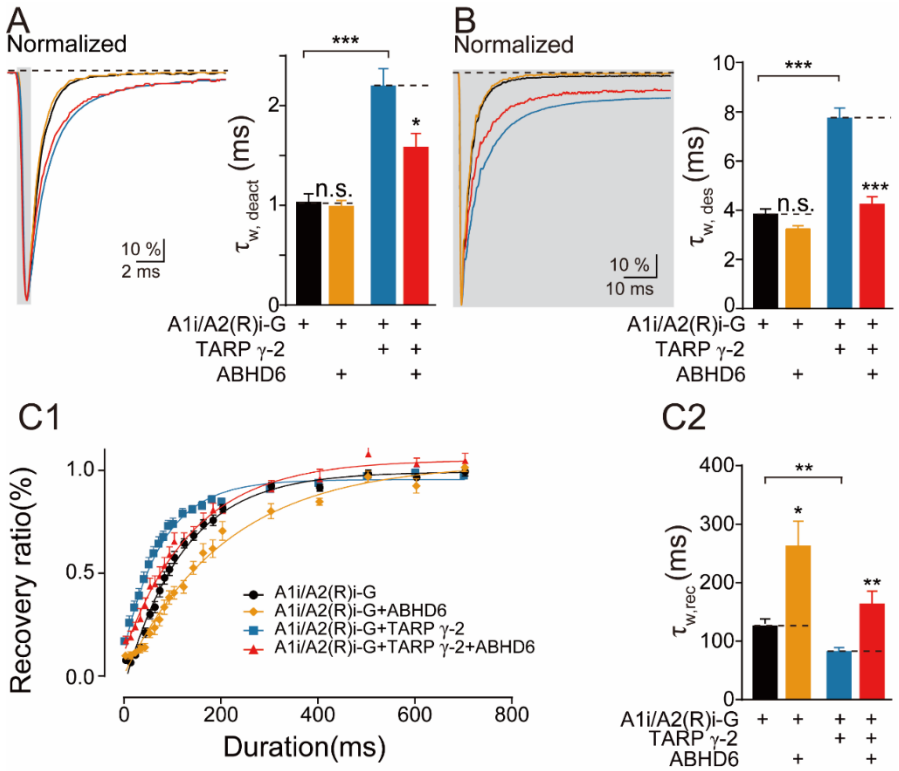

Figure 5. Overexpression of ABHD6 accelerated the deactivation and desensitization of GluA1i/GluA2(R)i-G receptors-TARP γ-2 complexes in HEK 293T cells, slowed the recovery of GluA1i/GluA2(R)i-G receptors in the presence and absence of TARP γ-2.

(A) The normalized traces and the summary bar graphs of the $\tau_{w,\ deact}$ of Glutamate (10 mM Glu, 1 ms) induced currents in the outside-out patch recorded at -60 mV from HEK 293T cells transfected with GluA1i/GluA2(R)i-G (black), GluA1i/GluA2(R)i-G + ABHD6 (orange), GluA1i/GluA2(R)i-G + TARP γ-2 (blue), and GluA1i/GluA2(R)i-G + TARP γ-2 + ABHD6 (red).

(B) The normalized traces and the summary bar graphs of the $\tau_{w,\ des}$ and peak amplitude of Glutamate (10 mM Glu, 100 ms) induced currents in the outside-out patch recorded at -60 mV from HEK 293T cells transfected with GluA1i/GluA2(R)i-G (black), GluA1i/GluA2(R)i-G + ABHD6 (orange), GluA1i/GluA2(R)i-G + TARP γ-2 (blue), and GluA1i/GluA2(R)i-G + TARP γ-2 + ABHD6 (red).

(C) Glutamate (Glu, 10 mM) induced currents in an outside-out patch excised from an HEK 293T cell transfected with GluA1i/GluA2(R)i-G (black), GluA1i/GluA2(R)i-G

744 + ABHD6 (orange), GluA1i/GluA2(R)i-G + TARP γ-2 (blue), and
745 GluA1i/GluA2(R)i-G + TARP γ-2 + ABHD6 (red). The first application of 100 ms
746 glutamate was followed by a second glutamate application at increasing pulse
747 intervals at -60 mV. The recovery ratio curves from desensitization (C1), and the
748 summary bar graphs of the $\tau_{w, rec}$ (C2).
749 The statistical method was one-way ANOVA followed by a two-way comparison (*P
750 < 0.05; ***P < 0.01; ***P < 0.001. Table. EV5.2)
751

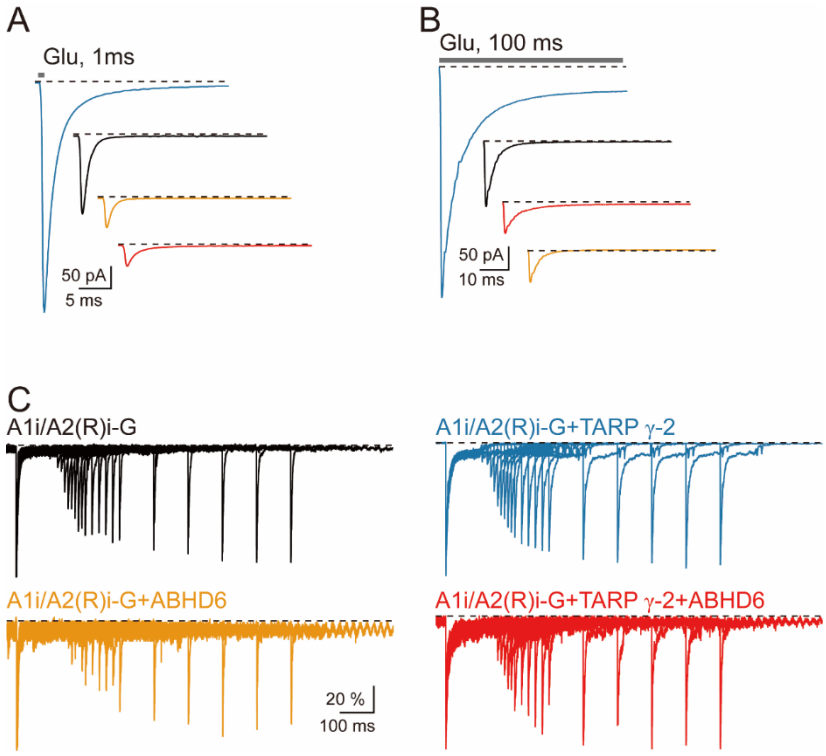

Figure EV5. Average traces of the deactivation, desensitization and recovery from desensitization of GluA1i/GluA2(R)i-G receptors-TARP γ-2 complexes in HEK 293T cells.

(A) The average traces of the $\tau_{w,\ deact}$ of Glutamate (10 mM Glu, 1 ms) induced currents in the outside-out patch recorded at -60 mV from HEK 293T cells transfected with GluA1i/GluA2(R)i-G (black), GluA1i/GluA2(R)i-G + ABHD6 (orange), GluA1i/GluA2(R)i-G + TARP γ-2 (blue), and GluA1i/GluA2(R)i-G + TARP γ-2 + ABHD6 (red).

(B) The average traces of the $\tau_{w,\ des}$ and peak amplitude of Glutamate (10 mM Glu, 100 ms) induced currents in the outside-out patch recorded at -60 mV from HEK 293T cells transfected with GluA1i/GluA2(R)i-G (black), GluA1i/GluA2(R)i-G + ABHD6 (orange), GluA1i/GluA2(R)i-G + TARP γ-2 (blue), and GluA1i/GluA2(R)i-G + TARP γ-2 + ABHD6 (red).

(C) The typical trace of recovery from desensitization. Glutamate (Glu, 10 mM) induced currents in an outside-out patch excised from an HEK 293T cell transfected with GluA1i/GluA2(R)i-G (black), GluA1i/GluA2(R)i-G + ABHD6 (orange), GluA1i/GluA2(R)i-G + TARP γ-2 (blue), and GluA1i/GluA2(R)i-G + TARP γ-2 +

770 ABHD6 (red). The first application of 100 ms glutamate was followed by a second
771 glutamate application at increasing pulse intervals at -60 mV.
772

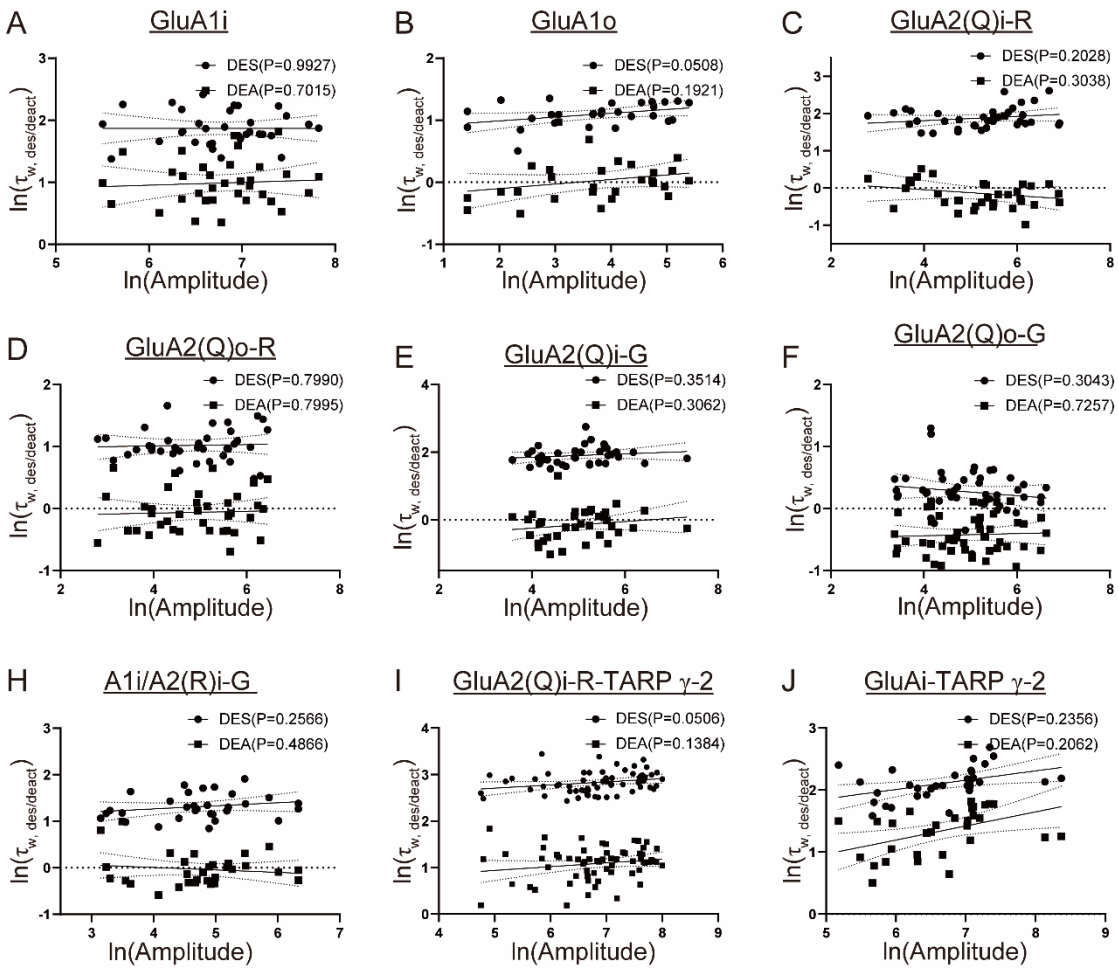

Figure EV6. Pearson's correlation between natural logarithm peak amplitude (pA) and the $\tau_{w,\ deact}$ and $\tau_{w,\ des}$ coexpression with various GluA subunits.

(A-J) Pearson's correlation and Local Polynomial Regression (loess) with 95% confidence intervals between natural logarithm peak amplitude (pA) and the $\tau_{w,\ deact}$ (ms) of Glutamate (10 mM Glu, 1 ms) induced currents and $\tau_{w,\ des}$ (ms) of Glutamate (10 mM Glu, 100 ms) induced currents in the outside-out patch from HEK 293T cells transfected with various GluA subunits.

783 Table EV1.1. Summary of peak amplitude(pA) of GluAs when co-transfected
784 with/without γ-2 or/and ABHD6.

Subnit	**GluA**	**GluA + ABHD6**	**GluA + TARP γ-2**	**GluA + TARP γ-2 + ABHD6**
GluA1i	226.69 ± 167.55(32)	77.91 ± 76.58(36)[a]	1005.89 ± 530.81(33)[a]	135.92 ± 140.83(36)[b]
GluA1o	88.67 ± 59.73(33)	42.62 ± 48.11(38)[a]	309.24 ± 211.47(37)[a]	115.51 ± 126.12(30)[b]
GluA2(Q)i-R	281.51 ± 256.66(36)	87.50 ± 81.75(42)[a]	911.62 ± 607.39(38)[a]	77.86 ± 157.14(44)[b]
GluA2(Q)o-R	201.23 ± 171.09(38)	63.84 ± 95.32(46)[a]	736.02 ± 579.63(34)[a]	82.15 ± 205.29(41)[b]
GluA2(Q)i-G	211.76 ± 254.32(38)	95.45 ± 119.83(38)[a]	660.77 ± 389.82(38)[a]	42.89 ± 59.48(43)[b]
GluA2(Q)o-G	196.15 ± 175.99(48)	41.57 ± 39.21(45)[a]	567.72 ± 361.19(46)[a]	37.75 ± 56.79(49)[b]
GluA2(R)i-R	2.55 ± 3.32(26)	1.86 ± 1.27(30)	55.83 ± 52.57(39)[a]	5.34 ± 6.69(30)[b]
GluA2(R)o-R	1.72 ± 1.51(14)	1.72 ± 0.88(29)	28.69 ± 32.66(34)[a]	12.63 ± 19.49(26)[b]
GluA2(R)i-G	2.60 ± 3.59(33)	2.55 ± 2.56(33)	31.32 ± 35.76(36)[a]	3.29 ± 4.82(33)[b]
GluA2(R)o-G	2.57 ± 2.41(43)	1.95 ± 1.62(49)	9.26 ± 9.75(48)[a]	1.95 ± 1.52(49)[b]
GluA3i-R	21.11 ± 40.80(26)	3.29 ± 5.57(20)	24.28 ± 46.24(25)	1.22 ± 1.15(21)b
GluA3o-R	6.10 ± 5.89(25)	2.46 ± 2.27(20)	11.38 ± 15.56(25)	4.36 ± 11.04(21)[b]
GluA3i-G	9.83 ± 16.73(25)	3.32 ± 4.01(19)	15.27 ± 17.49(26)[a]	3.25 ± 2.83(19)[b]
GluA3o-G	3.12 ± 4.66(25)	1.15 ± 0.67(20)	4.70 ± 7.75(26)	1.15 ± 0.95(20)[b]
GluA2(Q)i-R-TARP γ-2	3.23 ± 1.15(73)	2.34 ± (73)	1.27 \	\
GluA1i-TARP γ-2	4.19 ± 1.69(36)	2.31 ± (36)	1.11 \	\
GluA2(Q)i-R-TARP γ-2 (+ 50 mV)	2.81 ± 1.80(74)	1.71 ± 0.93(71)	\	\
GluA1i-TARP γ-2 (+ 50 mV)	2.64 ± 1.23(36)	1.86 ± 1.05(36)	\	\

785 Mean (± S.D.) values for thepeak amplitude of glutamate-induced currents which
786 were calculated from the desensitization curves. And the curves from a double
787 exponential function fits to the glutamate-induced currents evoked by 100 ms
788 applications of 10 mM glutamate. Currents were recorded in outside-out patch

recordings (-60 mV) from cells transfected with GluA, GluA + ABHD6, GluA + TARP γ-2, GluA + TARP γ-2 + ABHD6. The number of patches is given in parenthesis.

[a]Significantly different from GluA.

[b]Significantly different from GluA + TARP γ-2.

796 Table EV1.2. Summary of P values for comparison of peak amplitude.

Subnit	**GluA+ABHD6 vs. GluA**	**GluA+TARP γ-2 vs. GluA**	**GluA+TARP γ-2+ABHD6 vs. GluA+TARP γ-2**
GluA1i	P=0.0037(**)	P<0.0001(***)	P<0.0001(***)
GluA1o	P=0.0143(*)	P<0.0001(***)	P<0.0001(***)
GluA2(Q)i-R	P=0.0045(**)	P=0.0009(***)	P<0.0001(***)
GluA2(Q)o-R	P=0.0001(***)	P=0.0018(**)	P<0.0001(***)
GluA2(Q)i-G	P=0.0070(**)	P=0.0003(***)	P<0.0001(***)
GluA2(Q)o-G	P<0.0001(***)	P=0.0008(***)	P<0.0001(***)
GluA2(R)i-R	P>0.9999(-)	P<0.0001(***)	P<0.0001(***)
GluA2(R)o-R	P>0.9999(-)	P<0.0001(***)	P=0.0485(*)
GluA2(R)i-G	P>0.9999(-)	P<0.0001(***)	P<0.0001(***)
GluA2(R)o-G	P=0.1356(-)	P<0.0001(***)	P<0.0001(***)
GluA3i-R	P=0.0007(-)	P>0.9999(-)	P<0.0001(***)
GluA3o-R	P=0.0775(-)	P>0.9999(-)	P=0.0028(**)
GluA3i-G	P>0.9999(-)	P=0.0066(**)	P=0.0005(***)
GluA3o-G	P>0.9999(-)	P=0.0838(-)	P=0.0002(***)
GluA2(Q)i-R-TARP γ-2	P<0.001(***)	\	\
GluA1i-TARP γ-2	P<0.001(***)	\	\
GluA2(Q)i-R-TARP γ-2 (+ 50 mV)	P<0.001(***)	\	\
GluA1i-TARP γ-2 (+ 50 mV)	P<0.001(***)	\	\

797 P values for comparison of peak amplitude of GluAs when co-transfected
798 with/without γ-2 or/and ABHD6.The data were analyzed using Prism 8 (GraphPad
799 Software), and each p values was adjusted to account for multiple comparisons.
800
801

802 Table EV2.1. Summary of $\tau_{w,\ deact}$ (ms) of GluAs when co-transfected with/without γ-
803 2 or/and ABHD6.

Subnit	**GluA**	**GluA + ABHD6**	**GluA + TARP γ-2**	**GluA + TARP γ-2 + ABHD6**
GluA1i	0.99 ± 0.21(32)	0.98 ± 0.41(36)	2.88 ± 1.16(33)[a]	1.38 ±0.38(36)[b]
GluA1o	1.09 ± 0.27(33)	1.00 ± 0.35(36)	1.91 ± 0.81(37)[a]	1.25 ± 0.49(30)[b]
GluA2(Q)i-R	1.03 ± 1.05(36)	1.15 ±0.77(43)	3.68 ± 3.13(38)[a]	1.78 ± 1.39(43)[b]
GluA2(Q)o-R	0.97 ± 0.40(38)	1.07 ± 0.42(47)	2.78 ± 1.43(34)[a]	1.66 ± 0.95(46)[b]
GluA2(Q)i-G	0.96 ± 0.55(37)	0.81 ± 0.37(38)	2.44 ± 1.46(38)[a]	1.79 ± 1.26(44)
GluA2(Q)o-G	0.68 ± 0.21(48)	0.76 ± 0.27(47)	1.90 ± 1.30(46)[a]	1.14 ± 0.60(50)[b]
GluA2(Q)i-R-TARP γ-2	17.47± 4.68(73)	11.78± 3.20(73)	\	\
GluA1i-TARP γ-2	8.78± 2.76(36)	5.80± 2.12(36)	\	\
GluA2(Q)i-R-TARP γ-2 (+ 50 mV)	15.52± 4.48(74)	10.31 ± 3.71(71)	\	\
GluA1i-TARP γ-2 (+ 50 mV)	6.81± 2.01(36)	5.64 ± 1.85(36)	\	\

804 Mean (± S.D.) values for the time constant of deactivation ($\tau_{w,\ deact}$). The deactivation
805 curves from a double exponential function fits to the glutamate-induced currents
806 evoked by 1 ms applications of 10 mM glutamate. Currents were recorded in outside-
807 out patch recordings (-60 mV) from cells transfected with GluA, GluA + ABHD6,
808 GluA + TARP γ-2, GluA + TARP γ-2 + ABHD6.The number of patches is given in
809 parenthesis.
810 [a]Significantly different from GluA.
811 [b]Significantly different from GluA + TARP γ-2.
812

Table EV2.2. Summary of P values for comparison of $\tau_{w,\ deact}$.

Subnit	**GluA+ABHD6 vs. GluA**	**GluA+TARP γ-2 vs. GluA**	**GluA+TARP γ-2+ABHD6 vs. GluA+TARP γ-2**
GluA1i	P>0.9999(-)	P<0.0001(***)	P<0.0001(***)
GluA1o	P>0.9999(-)	P<0.0001(***)	P=0.0005(***)
GluA2(Q)i-R	P>0.9999(-)	P<0.0001(***)	P=0.0003(***)
GluA2(Q)o-R	P>0.9999(-)	P<0.0001(***)	P=0.0012(**)
GluA2(Q)i-G	P>0.9999(-)	P<0.0001(***)	P=0.1473(-)
GluA2(Q)o-G	P>0.9999(-)	P<0.0001(***)	P=0.0005(***)
GluA2(Q)i-R-TARP γ-2	P<0.001(***)	\	\
GluA1i-TARP γ-2	P<0.001(***)	\	\
GluA2(Q)i-R-TARP γ-2 (+ 50 mV)	P<0.001(***)	\	\
GluA1i-TARP γ-2 (+ 50 mV)	P<0.001(***)	\	\

P values for comparison of $\tau_{w,\ deact}$ of GluAs when co-transfected with/without γ-2 or/and ABHD6.The data were analyzed using Prism 8 (GraphPad Software), and each p values was adjusted to account for multiple comparisons.

818 Table EV3.1. Summary of $\tau_{w, des}$ (ms) of GluAs when co-transfected with/without γ-2
819 or/and ABHD6.

Subnit	**GluA**	**GluA + ABHD6**	**GluA + TARP γ-2**	**GluA + TARP γ-2 + ABHD6**
GluA1i	2.91 ± 0.53(32)	2.59 ± 0.78(36)	6.72 ± 1.86(33)[a]	4.14 ± 1.35(36)[b]
GluA1o	3.39 ± 0.70(33)	2.90 ± 0.69(38)	5.52 ± 1.59(37)[a]	3.50 ± 1.15(30)[b]
GluA2(Q)i-R	6.82 ± 2.19(36)	6.26 ± 1.83(42)	15.43 ± 4.87(38)[a]	9.13 ± 3.41(44)[b]
GluA2(Q)o-R	2.82 ± 0.81(38)	2.66 ± 0.78(46)	4.71 ± 1.48(34)[a]	3.08 ± 1.33(41)[b]
GluA2(Q)i-G	7.00 ± 2.11(38)	6.25 ± 2.0(38)	15.85 ± 3.95(38)[a]	9.52 ± 3.93(43)[b]
GluA2(Q)o-G	1.36 ± 0.58(48)	1.36 ± 0.51(45)	2.01 ± 0.60(46)[a]	1.43 ± 0.50(49)[b]
GluA2(Q)i-R-TARP γ-2	17.47± 4.68(73)	11.78± 3.20(73)	\	\
GluA1i-TARP γ-2	8.78± 2.76(36)	5.80± 2.12(36)	\	\
GluA2(Q)i-R-TARP γ-2 (+ 50 mV)	15.52± 4.48(74)	10.31 ± 3.71(71)	\	\
GluA1i-TARP γ-2 (+ 50 mV)	6.81± 2.01(36)	5.64 ± 1.85(36)	\	\

820 Mean (± S.D.) values for time constant of desensitization ($\tau_{w, des}$) from the
821 desensitization curves. Currents were recorded in outside-out patch recordings (-60
822 mV) from cells transfected with GluA, GluA + ABHD6, GluA + TARP-γ-2, GluA +
823 TARP-γ-2 + ABHD6. The number of patches is given in parenthesis.
824 [a]Significantly different from GluA.
825 [b]Significantly different from GluA + TARP γ-2.
826

827 Table EV3.2. Summary of P values for comparison of $\tau_{w, des}$.

Subnit	**GluA+ABHD6 vs. GluA**	**GluA+TARP γ-2 vs. GluA**	**GluA+TARP γ-2+ABHD6 vs. GluA+TARP γ-2**
GluA1i	P>0.9999(-)	P<0.0001(***)	P=0.0004(***)
GluA1o	P=0.2467(-)	P<0.0001(***)	P<0.0001(***)
GluA2(Q)i-R	P>0.9999(-)	P<0.0001(***)	P<0.0001(***)
GluA2(Q)o-R	P>0.9999(-)	P<0.0001(***)	P<0.0001(***)
GluA2(Q)i-G	P>0.9999(-)	P<0.0001(***)	P<0.0001(***)
GluA2(Q)o-G	P=>0.9999(-)	P<0.0001(***)	P<0.0001(***)
GluA2(Q)i-R-TARP γ-2	P<0.001(***)	\	\
GluA1i-TARP γ-2	P<0.001(***)	\	\
GluA2(Q)i-R-TARP γ-2 (+ 50 mV)	P<0.001(***)	\	\
GluA1i-TARP γ-2 (+ 50 mV)	P=0.013(*)	\	\

828 P values for comparison of $\tau_{w, des}$ of GluAs when co-transfected with/without γ-2
829 or/and ABHD6.The data were analyzed using Prism 8 (GraphPad Software), and each
830 p values was adjusted to account for multiple comparisons.
831
832

Table EV4.1. Summary of $\tau_{w, rec}$ (ms) of GluAs when co-transfected with/without γ-2 or/and ABHD6.

Subnit	**GluA**	**GluA + ABHD6**	**GluA + TARP γ-2**	**GluA + TARP γ-2 + ABHD6**
GluA1i	223.90 ± 124.60(32)	225.00 ± 201.39(29)	80.66 ± 22.56(33)[a]	126.50 ± 58.83(30)[b]
GluA1o	182.60 ± 87.20(28)	165.60 ± 39.86(25)	100.70 ± 27.76(33)[a]	119.90 ± 41.56(26)
GluA2(Q)i-R	77.17 ± 41.26(36)	75.89 ± 32.54(38)	56.98 ± 17.86(42)[a]	66.44 ± 33.63(27)
GluA2(Q)o-R	67.60 ± 28.29(35)	68.87 ± 36.06(33)	54.05 ± 17.56(33)	59.95 ± 26.61(33)
GluA2(Q)i-G	52.29 ± 20.93(37)	56.23 ± 37.72(29)	40.85 ± 27.86(35)[a]	47.39 ± 26.72(31)
GluA2(Q)o-G	50.48 ± 16.68(44)	58.12 ± 33.49(39)	50.39 ± 18.40(45)	55.68 ± 29.88(35)
GluA2(Q)i-R-TARP γ-2	77.61± 20.99(63)	82.66± 20.75(63)	\	\
GluA1i-TARP γ-2	93.89± 22.90(36)	127.22± 11.96(36)	\	\

Mean (± S.D.) values for constant of recovery from desensitization ($\tau_{w, rec}$) from the recovery ratio curves, which were calculated using nonlinear one-phase exponential decay fitting. Currents were recorded in outside-out patch recordings (-60 mV, 10 mM glutamate; 100 ms) when performing two-pulse stimulation, from cells transfected with GluA, GluA + ABHD6, GluA + TARP γ-2, GluA + TARP γ-2 + ABHD6. The number of patches is given in parenthesis.

[a]Significantly different from GluA.

[b]Significantly different from GluA + TARP γ-2.

844 Table EV4.2. Summary of P values for comparison of $\tau_{w, rec}$.

Subnit	**GluA+ABHD6 vs. GluA**	**GluA+TARP γ-2 vs. GluA**	**GluA+TARP γ-2+ABHD6 vs. GluA+TARP γ-2**
GluA1i	P>0.9999(-)	P<0.0001(***)	P=0.0092(**)
GluA1o	P>0.9999(-)	P<0.0001(***)	P=0.4938(-)
GluA2(Q)i-R	P>0.9999(-)	P=0.0325(*)	P>0.9999(-)
GluA2(Q)o-R	P>0.9999(-)	P=0.1988(-)	P>0.9999(-)
GluA2(Q)i-G	P>0.9999(-)	P=0.0014(**)	P=0.8413(-)
GluA2(Q)o-G	P>0.9999(-)	P>0.9999(-)	P>0.9999(-)
GluA2(Q)i-R-TARP γ-2	P=0.075(-)	\	\
GluA1i-TARP γ-2	P<0.001(***)	\	\

845 P values for comparison of $\tau_{w, rec}$ of GluAs when co-transfected with/without γ-2
846 or/and ABHD6.The data were analyzed using Prism 8 (GraphPad Software), and each
847 p values was adjusted to account for multiple comparisons.
848

849 Table EV5.1. Summary of GluA1i/GluA2(R)i-G receptors when co-transfected
850 with/without γ-2 or/and ABHD6.

	GluA1i/GluA2(R)i-G	**GluA1i/GluA2(R)i-G + ABHD6**	**GluA1i/GluA2(R)i-G + TARP γ-2**	**GluA1i/GluA2(R)i-G + TARP γ-2 + ABHD6**
Peak amplitude	156.96 ± 140.07(31)	65.75 ± 66.79(33) [a]	492.72 ± 454.74(34)[a]	67.45 ± 141.71(32)[b]
$\tau_{w, deact}$	1.04 ± 0.46(31)	1.00 ± 0.30(33)	2.20 ± 0.98(34)[a]	1.59 ± 0.76(32)[b]
$\tau_{w, des}$	3.85 ± 1.10(31)	3.24 ± 0.76(33)	7.77 ± 2.27(34)[a]	4.27 ± 1.53(32)[b]
τ_{rec}	129.72 ± 39.79(23)	263.71 ± 180.45(19)[a]	83.11 ± 28.70(23)[a]	164.42 ± 86.02(17)[b]

851 Mean (± S.D.) values for peak amplitude, $\tau_{w, des}$ from the desensitization and $\tau_{w, deact}$,
852 from the deactivation curves, and τ_{rec} from the recovery ratio curves. Currents were
853 recorded in outside-out patch recordings (- 60 mV, 10 mM glutamate; 100 ms / 1 ms /
854 100 two-pulse stimulation) without spermine in internal solution, from cells
855 transfected with GluA1i/GluA2(R)i-G, GluA1i/GluA2(R)i-G + ABHD6,
856 GluA1i/GluA2(R)i-G + TARP γ-2, GluA1i/GluA2(R)i-G + TARP γ-2 + ABHD6. The
857 number of patches is given in parenthesis.
858 [a]Significantly different from GluA1i/GluA2(R)i-G.
859 [b]Significantly different from GluA1i/GluA2(R)i-G + TARP γ-2.
860

Table EV5.2. Summary of P values for comparison of GluA1i/GluA2(R)i-G receptors when co-transfected with/without γ-2 or/and ABHD6.

	GluA1i/GluA2(R)i-G +ABHD6 vs. GluA1i/GluA2(R)i-G	**GluA1i/GluA2(R)i-G +TARP γ-2 vs. GluA1i/GluA2(R)i-G**	**GluA1i/GluA2(R)i-G +TARP γ-2+ABHD6 vs. GluA1i/GluA2(R)i-G +TARP γ-2**
Peak amplitude	P=0.01(*)	Pp=0.007(**)	P<0.001 (***)
$\tau_{w,\ deact}$	P>0.99(-)	P<0.001(***)	P=0.03(*)
$\tau_{w,\ des}$	P=0.43(-)	P<0.001(***)	P<0.001(***)
τ_{rec}	P=0.0109(*)	P=0.0076(**)	P=0.0011(**)

P values for comparison of Peak amplitude, $\tau_{w,\ deact}$, $\tau_{w,\ des}$, τ_{rec} of GluA1i/GluA2(R)i-G when co-transfected with/without γ-2 or/and ABHD6. The data were analyzed using Prism 8 (GraphPad Software), and each p values was adjusted to account for multiple comparisons.